Kinetic modeling for palm oil epoxidation using genetics algorithm

Mohd Jumain Jalil[1,*], Alif Farhan Mohd Yamin[2], Khairul Azhar Kamal[1], Hamzah Hafizuddin[1], Muhammad Salman Samin[1]

[1)] Faculty of Chemical Engineering, Universiti Teknologi MARA Cawangan Pulau Pinang, 13500 Permatang Pauh, Pulau Pinang, Malaysia
[2)] Faculty of Mechanical Engineering, Universiti Teknologi MARA Cawangan Pulau Pinang, 13500 Permatang Pauh, Pulau Pinang, Malaysia

[*]Corresponding e-mail: mjumain0686@ppinang.uitm.edu.my

Keywords: Epoxidation; palm oil; kinetic study

ABSTRACT – In recent years, there are abundant of studies in epoxidation of vegetable oil, this is due to the rising demand for eco-friendly epoxide. As the epoxide is the important chemical precursor in the industry. So, kinetic model was being conducted in order to determine the optimum value of epoxidation process. Initial concentration of formic acid (FA), hydrogen peroxide (H_2O_2) and oleic acid (OA) were 1.4714 mol/L, 1.4714 mol/L and 2.9483 mol/L respectively. Hence, the kinetic rate obtained are k_{11} = 0.1334 mol.L/min, k_{21} = 0.0781 mol.L/min, k_{31} = 0.0163 mol.L/min, k_{51} = 0.0169 mol.L/min. The minimum error is 0.2724.

1. INTRODUCTION

Recently, epoxidized palm oil (EPO) is high in demand for its function as intermediate in production of paint and coating element [1]. It also happens because of rising in demand for eco-friendly product. According to Jumain [2], the palm oil is the type of vegetable oil which able to epoxidized because it contains unsaturated triglycerides. Epoxy ring-opening or epoxy ring degradation takes place in the epoxidation of vegetable oil as to control process in order to produce good yield and high peroxide values of EPO [3][4].

2. METHODOLOGY

Chemical reaction for formation of epoxide and degradation of epoxidation palm oil are shown below:

Formation of epoxide:

$$FA + H_2O_2 \underset{k12}{\overset{k11}{\rightleftarrows}} PFA + H_2O \quad (1)$$

$$PFA + OA \underset{k22}{\overset{k21}{\rightleftarrows}} EPOXY + FA \quad (2)$$

Degradation of EPO:

$$EPOXY + H_2O \underset{k32}{\overset{k31}{\rightleftarrows}} DHSA \quad (3)$$

$$EPOXY + H_2O_2 \underset{k42}{\overset{k41}{\rightleftarrows}} DEG1 \quad (4)$$

$$EPOXY + FA \underset{k52}{\overset{k51}{\rightleftarrows}} DEG2 \quad (5)$$

Where, FA is formic acid, H_2O_2 is hydrogen peroxide, PFA is performic acid, H_2O is water, OA is oleic acid, DHSA is dihydroxy stearic acid.

Computing ode45 function in MATLAB Simulation in order to determine the optimum kinetic reaction of epoxidation.

$$\frac{d[FA]}{dt} = -k_{11}[FA][H_2O_2] + k_{12}[PFA][H_2O] + k_{21}[PFA][OA] - k_{22}[EPOXY][FA] - k_{51}[EPOXY]FA] + k_{52}[DEG2] \quad (6)$$

$$\frac{d[H_2O_2]}{dt} = -k_{11}[FA][H_2O_2] + k_{12}[PFA][H_2O] \quad (7)$$

$$\frac{d[PFA]}{dt} = k_{11}[FA][H_2O_2] - k_{12}[PFA][H_2O] - k_{21}[PFA][OA] + k_{22}[EPOXY][FA] \quad (8)$$

$$\frac{d[H_2O]}{dt} = k_{11}[FA][H_2O_2] - k_{12}[PFA][H_2O] - k_{31}[H_2O][EPOXY] + k_{32}[DHSA] \quad (9)$$

$$\frac{d[OA]}{dt} = -k_{21}[PFA][OA] + k_{22}[EPOXY][FA] \quad (10)$$

$$\frac{d[EPOXY]}{dt} = k_{21}[PFA][OA] - k_{22}[EPOXY][FA] - k_{31}[EPOXY][H_2O] + k_{32}[EPOXY][H_2O] \quad (11)$$

$$\frac{d[DHSA]}{dt} = k_{31}[EPOXY][H_2O] - k_{32}[DHSA] \quad (12)$$

$$\frac{d[DEG1]}{dt} = k_{41}[EPOXY][H_2O_2] - k_{42}[DEG1] \quad (13)$$

$$\frac{d[DEG2]}{dt} = k_{51}[EPOXY][FA] - k_{52}[DEG2] \quad (14)$$

3. RESULTS AND DISCUSSION

The reaction rate, k of experimental data is corresponding to the initial concentration which are 1.4714 mol/L: 1.4714 mol/L: 2.9483 mol/L (FA:H_2O_2:OA). The result of k from the simulation are tabulated in Table 1.

Table 1 Estimated reaction rate, k from simulation.

Kinetic reaction, k	Value (mol. L/min)
k_{11}	0.1334
k_{21}	0.0781
k_{31}	0.0163
k_{51}	0.0169
Minimum error = 0.2724	

From Table 1, the k will be input into the MATLAB Simulation in order to the plot the experiment data and simulation data. The plot graph is shows in Figure 1.

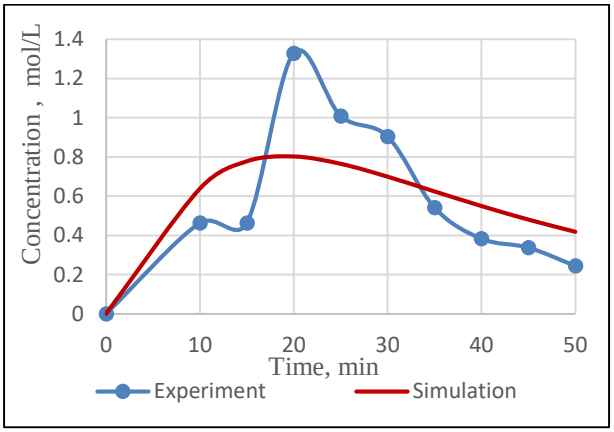

Figure 1 Comparison between experiment and simulation.

A comparison between experimental data and simulation based on kinetic reaction that obtained in Table 1 is plotted in Figure 1. From 0-20 min, it shows the formation of epoxide as the graph is increasing meanwhile from 20-50 min, the graph is decreasing, it shows the degradation of epoxidation is occurred. The simulation is deviated from experimental data as the simulation is solely depend on chemical equation and the reaction takes place at the same time. It is different from experimental as it takes a lot of other factor that influence the data. A mathematical model was developed by Leveneur et al., [5] to analyze an exothermic liquid-liquid reaction using epoxidation of oleic acid by performicacid *in situ* as example. The kinetics epoxidation of rubber seed oil (RSO) by peroxyacetic acid generated in situ were studied at various temperatures. This study was covered by Okiemen [6] and they found that epoxidation with almost complete conversion of unsaturated carbon and negligible oxirane cleavage can be attained by the in situ technique. The rate constant for epoxidation of RSO was found to be of the order of 10-6 mol-1 s-1 and activation energy of epoxidation of 15.7 kcal mol-1 was determined.

Figure 2 shows the reaction happen in epoxidation and degradation of epoxide process from MATLAB simulation. The simulation correctly predicted the reaction occur.

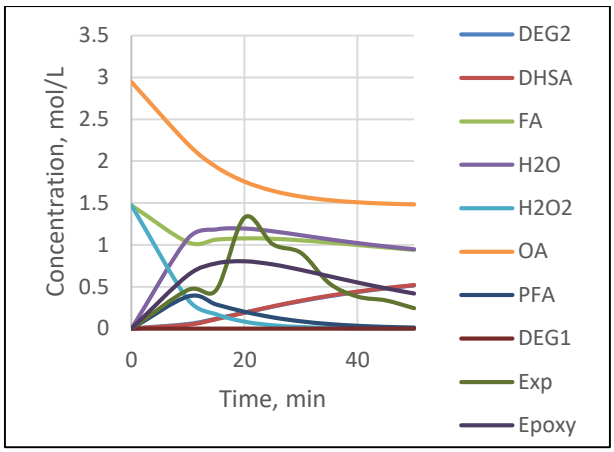

Figure 2 Concentration on each reaction.

4. CONCLUSION

Thus, the simulated kinetic model successfully represents the experiment data. Therefore, the kinetic reaction obtained from the simulation are k_{11} = 0.1334 mol.L/min, k_{21} = 0.0781 mol.L/min, k_{31} = 0.0163 mol.L/min, k_{51} = 0.0169 mol.L/min. Besides, the minimum error that generated by genetic algorithm is 0.2724. From the minimum error value, it indicates that the simulation is acceptable.

REFERENCES

[1] Jalil, A. Farhan, M. Yamin, S. H. Chang, I. S. Azmi, and N. Morad (2018). Selective epoxidation of crude oleic acid-palm oil with in situ generated performic acid. *International Journal Engineering and Technology*, *7*(2), 152–155.

[2] Jalil, S. K., Jamaludin, A., Rafizan (2018). Degradation Oxirane ring kinetics of epoxidized palm kernel oil- based crude oleic acid. *Chemistry and Chemical Technology*, *12*(3) 296–299.

[3] Campanella, A., & Baltanás, M. A. (2005). Degradation of the oxirane ring of epoxidized vegetable oils in liquid-liquid systems: I. Hydrolysis and attack by H_2O_2. *Latin American applied research*, *35*(3), 205-210.

[4] Vanags, M. Kirpluks, U. Cabulis, and Z. Walterova (2018). Highly Functional polyol synthesis from epoxidized tall oil fatty acids. *Journal of Renewable Materials, 4*(12), 1–8.

[5] Leveneur, A. Ledoux, L. Estel, B. Taouk, and T. Salmi (2014). Epoxidation of vegetable oils under microwave irradiation. *Chemical Engineering Research and Design*, *2*(11), 1495–1502.

[6] Okieimen, O. I. Bakare, and C. O. Okieimen (2002). Studies on the epoxidation of rubber seed oil. *Industrial Crops and Products*, *15*(1), 139–144.

Comparative study of modeling method of synthetic-jet-assisted mixing

Hong Mun Hoh[1], Cheng See Yuan[2,*], Lim Kim Chuan[3]

[1)] Fakulti Kejuruteraan Mekanikal, Universiti Teknikal Malaysia Melaka,
Hang Tuah Jaya, 76100 Durian Tunggal, Melaka, Malaysia
[2)] Centre for Advanced Research on Energy, Universiti Teknikal Malaysia Melaka,
Hang Tuah Jaya, 76100 Durian Tunggal, Melaka, Malaysia
[3)] Centre for Telecommunication Research & Innovation, Universiti Teknikal Malaysia Melaka,
Hang Tuah Jaya, 76100 Durian Tunggal, Melaka, Malaysia

[*]Corresponding e-mail: cheng@utem.edu.my

Keywords: Numerical modelling; synthetic jet; mixing

ABSTRACT – The aim of the present study is to compare the mixing performance of 2D and 3D Computational Fluid Dynamics (CFD) models of synthetic-jet-assisted fluid mixer. Both geometric models which consist of a mixing channel with a pair of synthetic jet actuators were generated. The diaphragm motion of the synthetic jet actuators was realized by a moving mesh method. Mixing degree was numerically predicted as the result of the CFD models. The results were validated against experimental data. The study concludes that the 3D model shows a better agreement against the experimental result than the 2D model.

1. INTRODUCTION

A synthetic jet is a zero-net-mass-flux (ZNMF) jet, which can be generated by the synthetic jet actuator (SJA). The actuator has a closed volume cavity with an oscillating diaphragm attached at one side and an orifice on the other. Due to the oscillating motion of the diaphragm, the processes of expulsion and ingestion of fluid are created around the orifice exit. Thus, a train of vortical structures are produced interact with the ambient fluid before entraining them into the jet. Lately, some numerical studies have been carried out to investigate the mixing efficiency between different fluids in micromixers [1-3]. However, high computation cost might become a drawback for the numerical approaches as compared to the experimental approaches. Comparing to the 3D model, numerical approaches by a 2D model helps to reduce the computation cost due to lower mesh density. Yet, the difference between the mixing degree obtained from a 2D and 3D CFD model remains questionable due to limited reporting in the literature. Therefore, the aim of the present study is to compare the mixing performance of 2D and 3D CFD model of synthetic-jet-assisted fluid mixer in view that the outcome of the study could serve as a guideline of modeling of such fluid mixer.

2. METHODOLOGY

For the stated objectives, a commercial CFD software ANSYS, Inc is used to simulate all the cases. Viscous laminar model is applied to all the cases. The geometric model of the synthetic jet actuator (SJA) is created by using ANSYS DesignModuler (as shown in Figure 1 & 2). Both models have the similar parametric conditions. Next, grid is created on the geometric model. ANSYS Fluent is utilized to solve the transient numerical simulation of the meshed model. Since the mixing performance of the fluid mixer is depending on the mixing degree between two fluids, hence, the mixing degree is numerically predicted as the result of the CFD models. By comparing the time-averaged mixing degree, the model is validated against the previous experimental study [4]. Notice that the experimental study [4] was conducted in 3D.

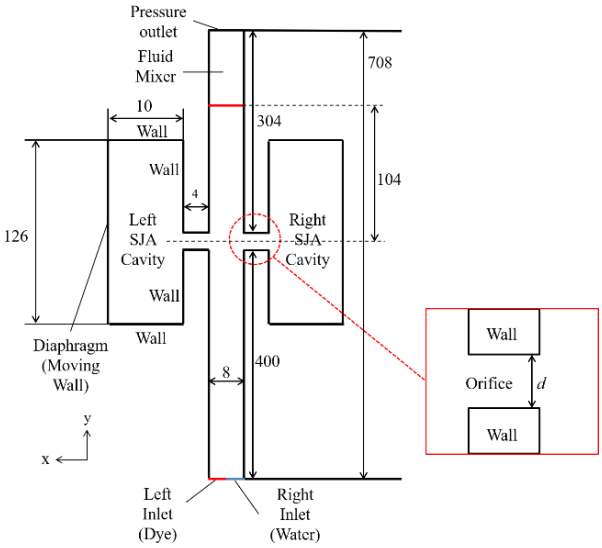

Figure 1 2D-Schematic diagram of the geometric model.

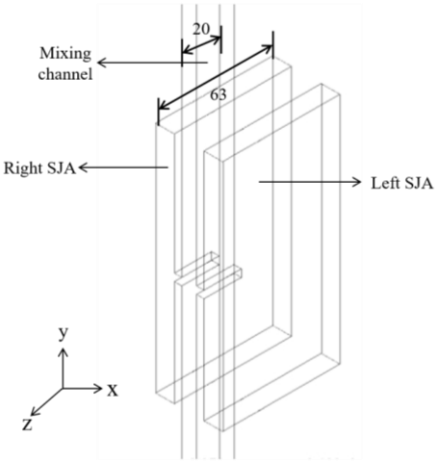

Figure 2 3D-Schematic diagram of the geometric model.

3. RESULTS AND DISCUSSION

As observed in Table 1, the 3D model slightly over predicted the mixing degree as compared to the experimental value. However, the agreement is deemed satisfactory. One the other hand, the mixing degree estimated from the 2D model is significantly lower than the experimental value.

Table 1 Comparison of mixing degree obtained from 2D and 3D model against the experimental data.

Model type	Present Mixing Degree	Exp Mixing Degree [5]	1/St
2D	0.07	0.677	0.3
3D	0.81	0.677	0.95

Figure 3 shows the instantaneous concentration contours from the experiment and the cases of 2D and 3D models. No mixing is attained in the case of 2D model as evidenced by concentrated red and blue contour on the left and right flow stream respectively. For the case with 3D model, similar flow patterns of the vortex structures are observed as compared to the one in the experimental study (as observed in Figure 3).

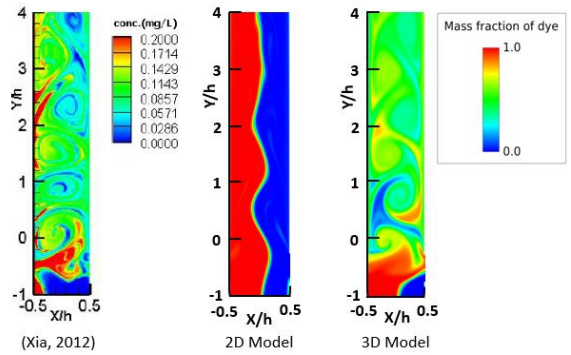

Figure 3 Comparison of instantaneous concentration contours around orifice exit region among experiment and two models (2D and 3D). Notice that the visualization results are captured at the end of the ejection cycle of left SJA.

Figure 4 compares the phase-averaged velocity vector fields and vorticity contours around the orifice exit region. As depicted, the jet does not form in the case of 2D model when the fluid is ejected from the orifices. For the 3D model, the vortices ejected from the orifices behave similarly to the one in the experimental flow visualization results. This phenomenon can be explained by the jet formation criterion proposed by the previous numerical and experimental studies [5] which reported that the jet formation criterion constant, K is approximately 1 and 0.16 for two-dimensional and axisymmetric synthetic jets, respectively. It is also shown that the jet formation criterion is governed by the equation, $\frac{1}{St} = \frac{Re}{S^2} > K$ where, St = Strouhal number, Re = Reynolds number and S = Stoke number. By referring to Table 1, the values of 1/St obtained from the 2D model is smaller than the jet formation criterion constant (K = 1). Therefore, no jet can be observed from the case with 2D model and subsequently leads to lower mixing degree between two fluids in the fluid mixer.

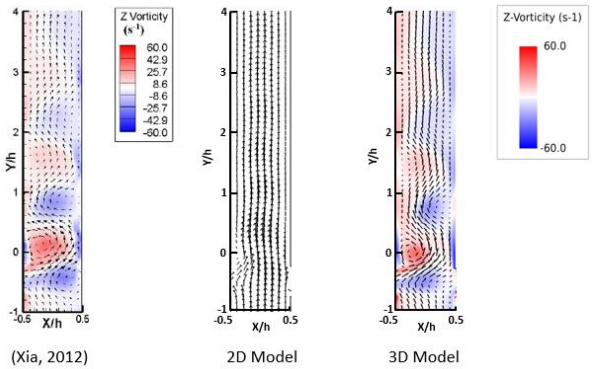

Figure 4 Comparison of phase-averaged velocity vector fields and vorticity contours around orifice exit region among experiment and two models (2D and 3D). Notice that the visualization results are captured at the end of the ejection cycle of left SJA.

4. CONCLUSION

A comparison between 2D and 3D numerical modeling of synthetic-jet-assisted mixing has been numerically investigated. The overall result showed that the approaches of using 2D and 3D model affected the mixing degree significantly. While the 3D model shows good agreement with the experimental result, the use of 2D model is proven ineffective for modeling of low Reynolds number synthetic-jet-assisted mixer due to relatively high jet formation criterion for 2D modeling.

ACKNOWLEDGEMENT

This project is supported by Universiti Teknikal Malaysia Melaka (UTeM) and Ministry of Higher Education Malaysia under FRGS/2018/FKM-CARe/F00375.

REFERENCES

[1] Cao, Q., Han, X., & Li, L. (2015). An active microfluidic mixer utilizing a hybrid gradient magnetic field. *International Journal of Applied Electromagnetics and Mechanics*, *47*(3), 583-592.

[2] Liu, K., Yang, Q., Chen, F., Zhao, Y., Meng, X., Shan, C., & Li, Y. (2015). Design and analysis of the cross-linked dual helical micromixer for rapid mixing at low Reynolds numbers. *Microfluidics and nanofluidics*, *19*(1), 169-180.

[3] Chen, X., & Li, T. (2016). A novel design for passive misscromixers based on topology optimization method. *Biomedical microdevices*, *18*(4), 57.

[4] Xia, Q. (2012). *Enhancement of liquids mixing using active pulsation in the laminar flow regime* (Doctoral dissertation, The University of Manchester (United Kingdom).

[5] Holman, R., Utturkar, Y., Mittal, R., Smith, B. L., & Cattafesta, L. (2005). Formation criterion for synthetic jets. *AIAA Journal*, *43*(10), 2110-2116.

MyPhysio – A proposed telephysiotherapy system to reduce patient hospital waiting time and improve patient monitoring

Lee Pik Yun, Raja Rina Raja Ikram*

Fakulti Teknologi Maklumat dan Komunikasi, Universiti Teknikal Malaysia Melaka,
Hang Tuah Jaya, 76100 Durian Tunggal, Melaka, Malaysia

Corresponding e-mail: raja.rina@utem.edu.my

Keywords: Telemedicine; rehabilitation; physiotherapy

ABSTRACT - This paper presents MyPhysio, a proposed online physiotherapy rehabilitation system with telemedicine-based consultation service to allow patients eliminate the hassle of regular trips and long wait at hospital center. Requirements elicitation was conducted with 30 patients and 12 physiotherapists to collect critical features and survey previous experiences with telemedicine. MyPhysio, a telemedicine system, was developed based on the results of the requirements elicitation.

1. INTRODUCTION

In Malaysia, patients have to undergo long waiting times for physiotherapy in the hospitals with others patients. As survey carry out by Cheema, R.K. in 2017 showed that 40.02% of patients wait up to 4 hours to seek a doctor and 26.3% of patients stop look for medical treatment due to long queueing time [4]. In Malaysian government hospitals, patients can wait up to two months to open a new case due to long queues as the services are offered at a cheaper price than private hospitals [1].

This situation causes inconvenience and frustration for patients that have serious musculoskeletal based injury [3]. Besides, physiotherapist also face difficulty in keeping up to date on patients' case if patients skip appointment. Furthermore, patients are not aware about the importance of carry out physiotherapy treatment which help them recovery faster in the right way [1].

Thus, telemedicine is shall be able to provide access to physiotherapy services in the comfort of the patient's home. Telemedicine allow healthcare providers to evaluate patients' condition regardless of where they are located [5,6].

2. RELATED WORKS

Figure 1 showed the comparison between proposed system MyPhysio with existed system in Malaysia such as Door2Door, TELEME and Doctor2U application. MyPhysio mainly focused on telemedicine, hospital appointment, electronic medical record and rehabilitation function that mostly requested by the patients and physiotherapist. Doctor2u provides an e commerce platform together with their application. However, the e commerce platform is deemed not necessary to be included in telephysiotherapy application as there are many platforms out there such as Shopee and Lazada. Door2door and TELEME system both also have limited features such as appointment scheduling and limited telemedicine using a web-based system. MyPhysio, our proposed application contains major functions that are required by patients and can be accessed via mobile devices. MyPhysio is one of the only applications that have access to web based and mobile devices, enabling more accessibility opportunities.

Features / System	Platform	Home Care service	E-Commerce	Telemedicine	Hospital Appointment	Electronic Medical Record	Rehabilitation System
MYPhysio	Web Based + Android			✓	✓	✓	✓
Door2Door (2014)	Web Based	✓					
TELEME (2016)	Web-based			✓			
Doctor2U (2015)	Web Based+Android + IOS	✓	✓	✓		✓	

Figure 1 MYPhysio versus existed system.

3. METHODOLOGY

Requirement elicitation was done through two set of questionnaires involving thirty patients and twelve physiotherapists to obtain feedback on the issues below:

(a) Experiences and opinions on current physiotherapy services
(b) Features that are important to be implemented in telephysiotherapy

4. RESULTS

A total of twenty out of thirty patients (66.7%) agreed they would accept telemedicine as a means of communication for follow up physiotherapy sessions and eight participants were neutral about it. Only two participants of 6.7% did not agree using telemedicine during doctor patient consultations, particularly during follow up sessions. Based on physiotherapists feedback, eight out of twelve patients (66.67%) agreed that telemedicine can improve patient access, patient experience and reduce patients from not attending scheduled physiotherapy appointments. Thus, it is worth to note that the use of telehealth application during physiotherapy can continue to provide quality services for patients.

The main features highlighted by participants to be included in the telephysiotherapy application are hospital appointments, physiotherapy session video uploads, speech to text command feature and emergency call.

4.1 Current Framework

Figure 2 showed the flowchart of current system used in hospital when a patient meets a physiotherapist.

We can observe that patient took time to register and wait in different department in order to receive physiotherapy treatment. This not only inconvenient for patients with serious musculoskeletal based injury, but also decrease hospitals' productivity.

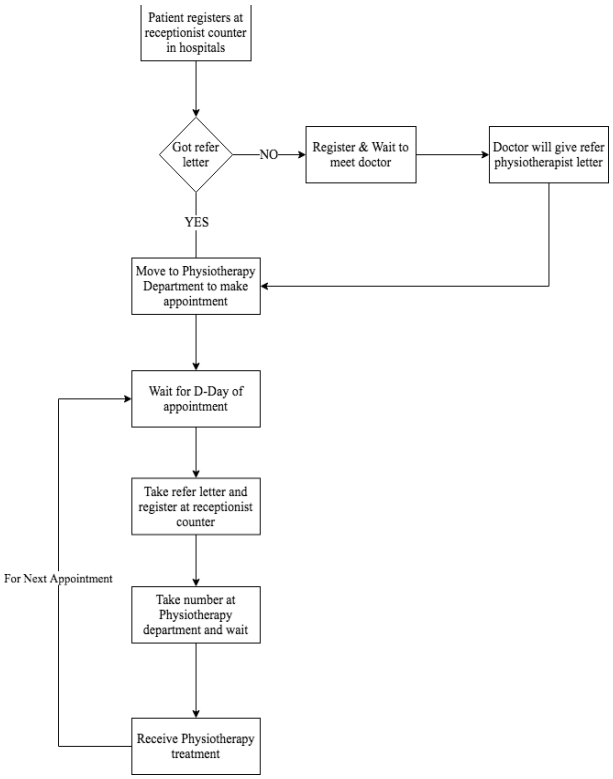

Figure 2 Flowchart of current system.

4.2 Proposed System-MyPhysio

Figure 3 shows the process flow of MyPhysio, an online physiotherapy rehabilitation system. There are three main users of the system – patient, admin and physiotherapist. The patient is required to have a first meeting with the physiotherapist before registering to use MyPhysio. Registered patients can make appointments and carry out telemedicine consultations according to schedule. They are also able to make online payments for consultations, rate the physhiotherapist chosen, make appoinments and access personalised health record. In addition, they are able to manage their own profile. After the first meeting with physiotherapist, the physiotherapist can design proper practice based on patient condition and provide feedback for every session.

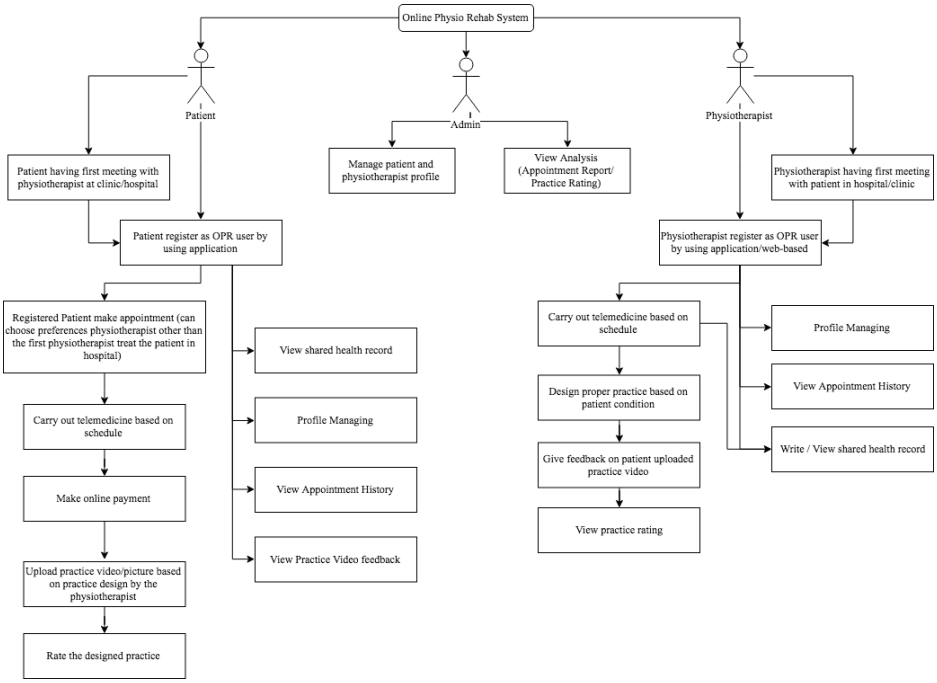

Figure 3 Proposed system MyPhysio.

5. CONCLUSION

In conclusion, MyPhysio proposed to allow patients eliminate the hassle of regular trips to hospital or physiotherapy center. In addition, it also enables monitoring of patients' health status to be done online by physiotherapists.

REFERENCES

[1] Ikram, R. R. R., Ghani, M. K. A., & Abdullah, N. (2015). An analysis of application of health informatics in Traditional Medicine: A review of four Traditional Medicine Systems. *International Journal of Medical Informatics*, *84*(11), 988-996.

[2] Ikram, R. R. R., Ghani, M. K. A., Ab Hamid, N. R., & Salahuddin, L. (2018). Enabling Ehealth in traditional medicine: a systematic review of information systems integration requirements. *Journal of Engineering Science and Technology*, *13*(12), 4193-4205.

[3] Afza, F., (2017). Major challenges the physiotherapy profession faces in expanding its role in health, prevention, and wellness services. *Journal Physiotherapy & Physical Rehabilitation*, *2*(4), pp. 1-3.

[4] Ahmad, B. A., Khairatul, K., & Farnaza, A. (2017). An assessment of patient waiting and consultation time in a primary healthcare clinic. *Malaysian family physician: the official journal of the Academy of Family Physicians of Malaysia*, *12*(1), 14-21.

[5] Chanen, J. S. Foley survey shows surging telemedicine services across the health care spectrum, into foreign markets. Available online: https://www.foley.com/foley-survey-shows-surging-telemedicine-services-across-the-health-care-spectrum-into-foreign-markets-11-15-2017. Acessed on 12 April 2019.

[6] Cheema, R. K. Patients foregoing treatment due to long waiting time in Malaysia hospital service, survey reveals. Available online: https://today.mims.com/patients-foregoing-treatment-due-to-long-waiting-time-in-malaysian-hospital-service-survey-reveals. Accessed on 12 April 2019.

Multifractal analysis for durability predictive criterion of suspension coil spring signal

C.H. Chin[1,*], S. Abdullah[1], S.S.K. Singh[1], A.K. Ariffin[1], D. Schramm[2]

[1)] Centre for Integrated Design for Advanced Mechanical System (PRISMA), Faculty of Engineering & Built Environment, Universiti Kebangsaan Malaysia, 43600 UKM Bangi, Selangor, Malaysia
[2)] Departmental Chair of Mechatronics, University of Duisburg-Essen, 47057 Duisburg, Germany

[*]Corresponding e-mail: chuinhao90@gmail.com

Keywords: Fatigue life; adaptive neuro-fuzzy inference system; multifractality

ABSTRACT – This work presents the fatigue life predictive model of suspension spring based on multifractal properties of road excitations. Random road excitations often possess obvious multifractal properties attributed to the surface irregularities. Hence, modelling of the coil spring fatigue life based on the road multifractality is feasible. Adaptive Neuro-Fuzzy Inference System (ANFIS) was used to model the relationship between the fatigue life and road multifractality, giving an acceptable accuracy in fatigue life prediction. The ANFIS model contributed to an accurate assessment of coil spring fatigue life based on road multifractality.

1. INTRODUCTION

Fatigue failure is a common type of failure found in many automotive mechanical components. This is mainly because ground vehicles are continuously exposed to complex road excitations under variable speeds, loads, and road excitations. Some studies have remarked that the combined effects of corrosion and wear as well as continuous exposure to vibrational loading have cause fatigue failure in suspension coil spring. Fatigue failure of the suspension coil spring will affect the ride comfort and the vehicle control. This may result in serious road accident and risk the passengers' life. Therefore, durability assessment is a key element in the production of coil spring to fulfil the requirements concerning safety, durability, reliability, and comfort [1]. In current industrial practice, the time domain approach is commonly utilised due to its high accuracy. This requires the knowledge of the service load (the time history of strain, acceleration, or displacement) for fatigue life prediction.

Strain-life approach is one of the widely applied time-domain approaches to evaluate the durability of automotive components owing to its simplicity and acceptable accuracy. Nonetheless, the complex geometry of coil spring and equipment limitations render the strain histories acquisition of coil spring a challenging task [2]. Additionally, the time-domain approach often requires high experimental cost because this method need large amount of data to sufficiently represent the real-life loading conditions [3]. This eventually causes lengthy and expensive field tests [1]. Besides that, long strain histories also significantly increase the computational duration. To reduce the manufacturing cost, automotive manufacturers demand for an alternative to alleviate the need for strain measurements of coil springs in evaluations of their durability [2].

Multifractal properties of road excitations are closely related to the surface roughness and thus the road multifractality can be a durability predictive criterium of coil spring [4]. Therefore, the relationship between the road multifractality and coil spring durability need to be determined. This study presents the establishment of fatigue life predictive model based on road multifractality using Adaptive Neuro-Fuzzy Inference System (ANFIS). The trained ANFIS model will contribute to an accurate durability prediction of coil spring based on road multifractality.

2. METHODOLOGY

This study employed ANFIS modelling technique to develop the fatigue life predictive model for suspension coil spring. Figure 1 depicts the methodology flowchart.

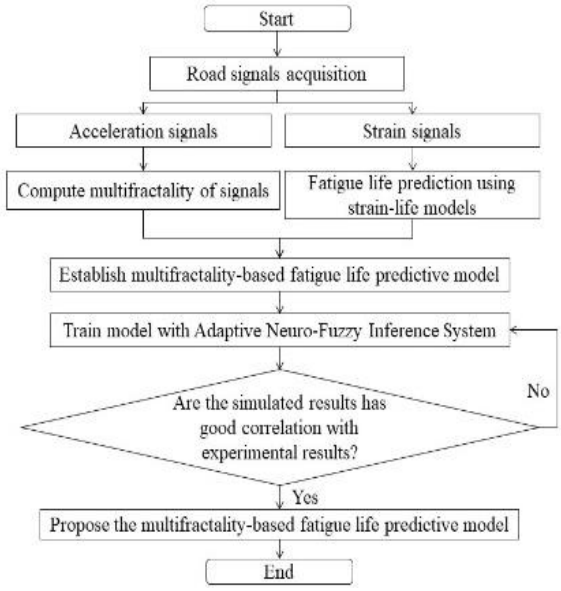

Figure 1 Formulation process of durability predictive model using ANFIS.

Acceleration and strain signals were acquired in road tests. Next, multifractal analysis was conducted on road acceleration signals to determine the singularity spectrum. The multifractality of signal was determined from the width of the spectrum. Morrow strain-life model was used to evaluate the fatigue life of coil springs. With the multifractality and fatigue live, a fatigue life predictive model was developed using ANFIS technique. During the training of the model, 90% input data was

used as the train data while another 10% was the checking data. Checking data was necessary to prevent the overfitting of the ANFIS model. Errors of the ANFIS model using checking data at each epoch of training were computed. Minimal checking error indicated least probability of overfitting. The root-mean-square-error (RMSE) is defined as:

$$RMSE = \sqrt{\frac{\sum_{n=1}^{N}(\hat{y}_n - y_n)}{N}} \quad (1)$$

Where $\hat{y}$ is predicted value, y is observed value and N is number of samples.

Finally, validation of the ANFIS model was done by correlating the simulated fatigue life with the experimental fatigue life.

3. RESULTS AND DISCUSSION

A fatigue life predictive model based on road excitations multifractality was trained using ANFIS modelling. During the training, it is important to monitor the checking root-mean-square-errors (RMSE) to prevent overfitting. Figure 2 shows the training and checking errors of the model during the training process. It was found that the training RMSE gradually decreased after each epoch, showing that the model is getting better fitted to the training data. However, the checking RMSE started to increase at epoch 8 of the training process. This indicates that the model became overfitted to the training data after epoch 8. Hence, the training process was then stopped at epoch 8 with the minimum difference of 24% with the training RMSE and lowest checking RMSE of 0.6953 to ensure the general use of the model.

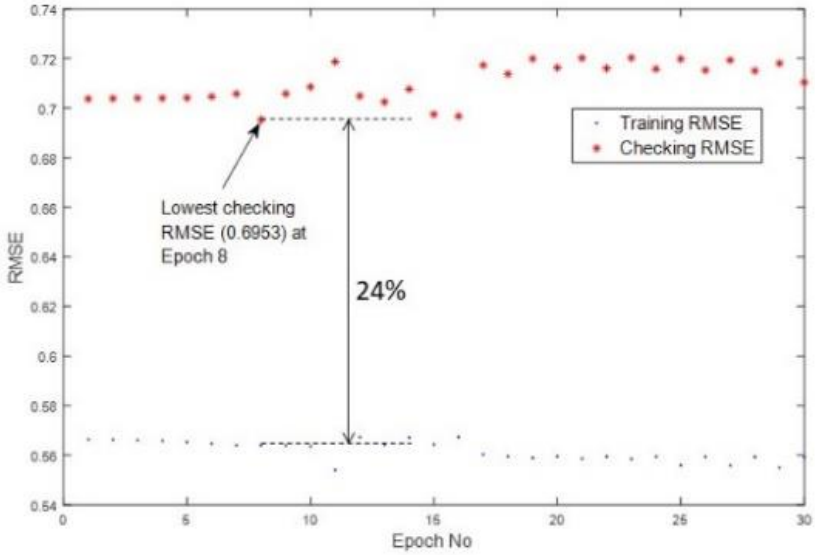

Figure 2 Training and checking RMSE of ANFIS model.

Figure 3 shows the outputs of the ANFIS model. The fatigue life of coil spring decreases as the road multifractality becomes higher. Road multifractality is closely related to the surface irregularities. A road with uneven surface contains irregularities like speed bumps, potholes or high surface roughness. The surface irregularities contributed to excessive vibration to the car body and caused fatigue damage to the coil spring. Quan et al. [4] proved that road surfaces possess obvious multifractal properties and the road multifractality increases with surface roughness. It is noteworthy that the fatigue life of coil spring constantly maintained at 10^4 cycles when the multifractality reached 0.5 and above. This shows that road signals with higher multifractality above 0.5 will have no significant effect on the fatigue life of coil spring.

The fatigue lives of coil spring simulated by the ANFIS model were correlated with the experimental fatigue lives as shown in Figure 4. It was shown that the simulated fatigue lives had a good conservative relationship with the experimental fatigue lives. 96% of data distributed within the acceptance boundaries between 1:2 and 2:1 correlation.

4. CONCLUSION

In this study, a fatigue life predictive model based on road multifractality was established. It was found that higher road multifractality resulted in lower fatigue life of coil spring. The fatigue life of coil spring remained at 10^4 cycles at the road multifractality of 0.5 and above. The trained model gave a good accuracy in fatigue life prediction since 96% of the simulated data had a good conservative relationship with the experimental results.

ACKNOWLEDGEMENTS

This work was financially funded by Universiti Kebangsaan Malaysia under the research grant GP-K007552. This work was also supported by the European Unions's Horizon 2020 research and innovation programme under the Marie Sklodowska-Curie grant agreement (No. 730888).

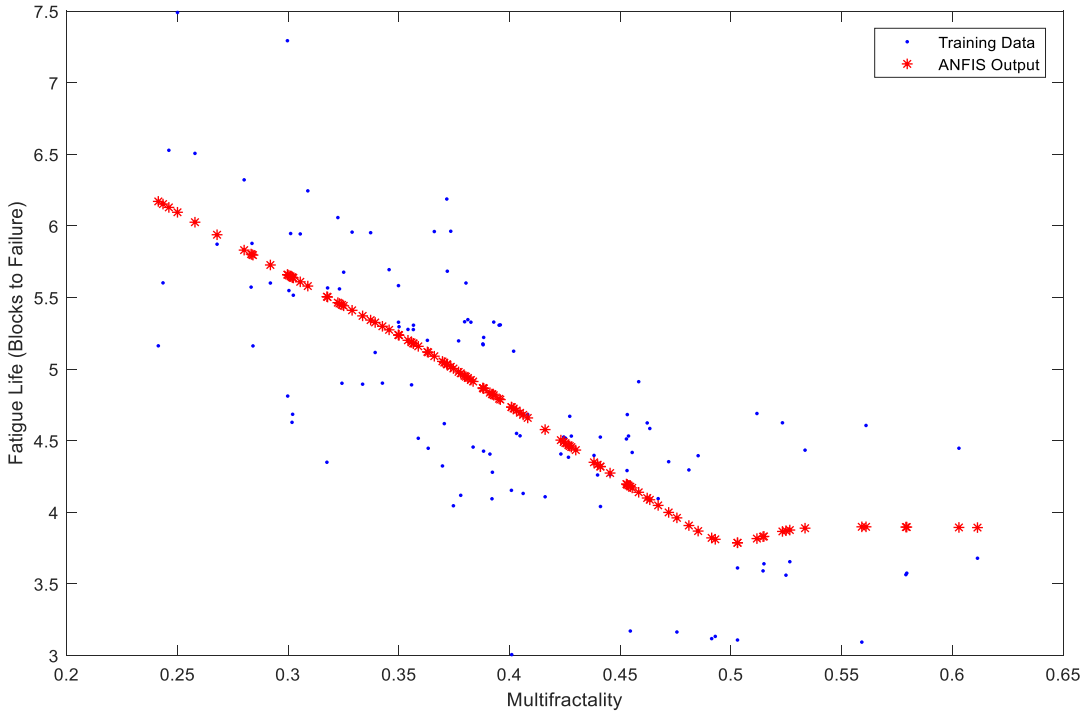

Figure 3 Output of ANFIS model.

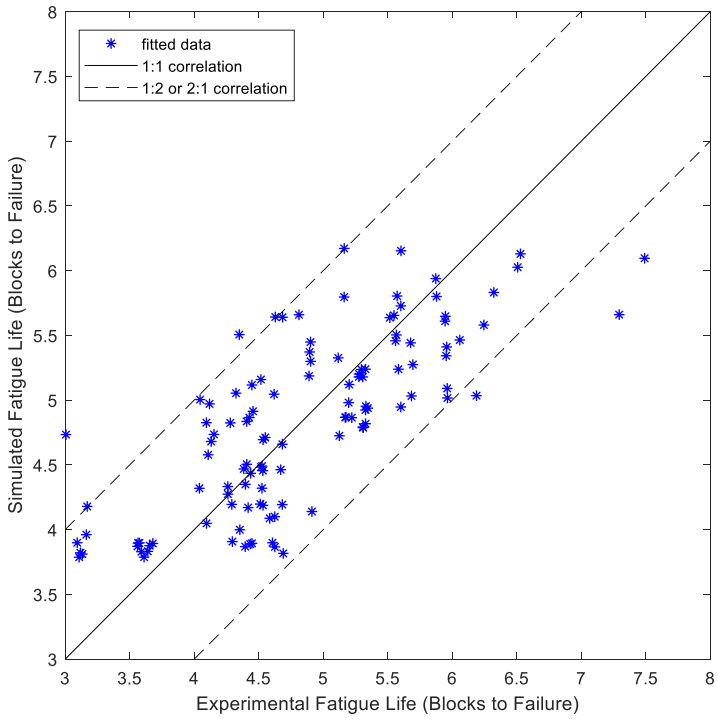

Figure 4 Relationship distribution between simulated and experimental fatigue lives.

REFERENCES

[1] Shafiullah, A. K. M. & Wu, C. Q. (2013). Generation and validation of loading profiles for highly accelerated durability tests of ground vehicle components. *Engineering Failure Analysis*, *33*, 1–16.

[2] Putra, T. E., Abdullah, S., Schramm, D., Nuawi, M. Z. & Bruckmann, T. (2017). The need to generate realistic strain signals at an automotive coil spring for durability simulation leading to fatigue life assessment. *Mechanical Systems and Signal Processing*, *94*, 432–447.

[3] Ugras, R. C., Alkan, O. K., Orhan, S., Kutlu, M. & Mugan, A. (2019). Real time high cycle fatigue estimation algorithm and load history monitoring for vehicles by the use of frequency domain methods. *Mechanical Systems and Signal Processing*, *118*, 290–304.

[4] Quan, W., Wang, H., Liu, X. & Zhang, S. (2013). Multi-fractal Analysis for Pavement Roughness Evaluation. *Procedia - Social and Behavioral Sciences, 96*, 2684–2691.

Modified Anand model parameters for 95.5Sn-4.0Ag-0.5Cu lead-free solder material

A.F.M. Yamin*, N.N. Azmi, N.A. Norrdin, H. Yusoff

Fakulti Kejuruteraan Mekanikal, Universiti Teknologi MARA, Cawangan Pulau Pinang, Kampus Permatang Pauh, 13500 Permatang Pauh, Pulau Pinang, Malaysia

*Corresponding e-mail: aliff.farhan6205@uitm.edu.my

Keywords: Solder joint; creep; Anand model

ABSTRACT – Anand model is often used to represent the deformation behavior of solder in an electronic package. To increase the capability of the model, two model parameters in the Anand model namely the initial value of state variable, $\boldsymbol{s_0}$ and hardening constant, $\boldsymbol{h_0}$ are modified. The 15 material parameters of the model for 95.5Sn-4.0Ag-0.5Cu (SAC405) were determined by a series of experimental data with 3 different test temperatures (25 °C, 75 °C and 150 °C) inelastic strain rates (10^{-5} s^{-1}, 10^{-4} $s^{-1,}$ and 10^{-3} s^{-1}). The comparison of the experimental and simulated results showed that the modified Anand model captured the simulation capability.

1. INTRODUCTION

Solder joints are extensively used in electronic industries to mount the electronic components into printed circuit boards (PCBs). It provides not only for electrical connections, but it includes the mechanical integrity and thermal dissipation. During system operation, the heat produced in the electronic components expands and shrinks the package assembly in different rates due to the variation of the material in the package. This mismatch of thermal expansion induces shear stress in the solder joints and subsequently fatigue failure when prolonged used. Since most of the electronics failure comes directly from the solder joint itself, thus, the study of the creep in the solder material is important. A unified constitutive model called Anand model [1 - 2] is widely used to predict the viscoplastic behaviors of the solder joints. But, the existing model had minor flawed since it cannot accurately predict in the strain-hardening for low-temperature applications. Thus, a modified Anand model was proposed to reduce this error [3]. This paper reports on the modified Anand model parameters extraction and its reliability to predict the inelastic behavior of the lead-free solder material namely 95.5Sn-4.0Ag-0.5Cu (SAC405) solder alloys. The material parameters for the constitutive model were taken out from available experimental data [4] and later as a validation purpose to capture the reliable response in terms of stress and inelastic strain.

2. UNIFIED CONSTITUTIVE EQUATION MODEL

Anand model is a phenomenological constitutive equation developed by Anand and Brown [1 - 2]. The model uses an internal state variable, s, to resist the inelastic flow at the local material point. The model is summarized as Equation (1), Equation (2) and Equation (3):

Flow Equation:

$$\dot{\varepsilon}_{in} = Ae^{-\frac{Q}{RT}}\left[\sinh\left(\zeta\frac{\sigma}{s}\right)\right]^{\frac{1}{m}} \quad (1)$$

Evolution of internal state variable, s:

$$\dot{s} = \left[h_0\left(1-\frac{s}{s^*}\right)^a \operatorname{sign}\left(1-\frac{s}{s^*}\right)\right]\dot{\varepsilon}_{in} \quad (2)$$

with:

$$s^* = \hat{s}\left(\frac{\dot{\varepsilon}_{in}}{A}e^{\frac{Q}{RT}}\right)^n \quad (3)$$

Where $\dot{\varepsilon}_{in}$ is inelastic strain rate, σ is equivalent stress and T is the temperature in absolute scale. Another definition of the model parameters is concluded in Table 1. In order to improve the existing model, the material parameters can be modified as a function of temperature and inelastic strain rate [3 - 4]. Two Anand model parameters were selected (s_0 and h_0) and modified accordingly as depicted in Equation (4) and Equation (5):

$$s_0 = c_0 + c_1T + c_2T^2 \quad (4)$$

$$h_0 = k_0 + k_1T + k_2T^2 + k_3\dot{\varepsilon}_{in} + k_4{\dot{\varepsilon}_{in}}^2 \quad (5)$$

3. DETERMINATION OF MODEL PARAMETERS

There are 15 material parameters of the modified Anand model and can be obtained through non-linear optimization methods from a series of stress-inelastic strain experiment data over a wide range of temperatures and inelastic strain rates. For determination of the parameters, the equivalent stress must be computed, and it's defined as:

$$\sigma = cs; \quad c < 1 \quad (6)$$

Whereby c is defined in Equation (7) as follow:

$$c = \frac{1}{\zeta}\sinh^{-1}\left[\left(\frac{\dot{\varepsilon}_{in}}{A}e^{\frac{Q}{RT}}\right)^m\right] \quad (7)$$

From Equation (2), the increment of the state variable, ds is calculated:

$$\mathrm{d}s = h_0\left(1-\frac{s}{s^*}\right)^a \mathrm{d}\varepsilon_{in}; \quad s < s^* \quad (8)$$

Integrate $s \to s_0$ to s and $\varepsilon_{in} \to 0$ to ε_{in}, respectively, yields:

$$s = s^* - \left\{[s^* - s_0]^{(1-a)} + (a-1)h_0[s^*]^{-a}\varepsilon_{in}\right\}^{\frac{1}{1-a}} \quad (9)$$

Substituting Equation (9) with Equation (6), the evolution of stress is summarized as Equation (10):

$$\sigma = c\left\{s^* - \left\{[s^* - s_0]^{(1-a)} + (a-1)h_0[s^*]^{-a}\varepsilon_{in}\right\}^{\frac{1}{1-a}}\right\} \quad (10)$$

The parameters extraction is started from the initial guess values within acceptable ranges found from published literature [3 - 4]. This is followed by the substitution of the predicted material parameters into Equations (3), (4), (5), (7) and (10). The accuracy of the model parameters is determined by minimizing the mean squared error (MSE) computed between the predicted stress in Equation (10) and actual stress from experimental data [4]. Since the model is highly non-linear, two stages optimization method was used. The first stage is a particle swarm optimization (PSO) technique with the aim of to search-space the region of global minimum of MSE. This is followed by a direct search method using the Nelder-Mead simplex algorithm to find optimal parameters based on the PSO results.

4. RESULTS AND DISCUSSION

Table 1 shows the results of the modified Anand model for SAC405 using optimization techniques discussed in Section 3. Based on the results from Table 1, the MSE computed is 0.589.

Table 1 Modified Anand parameters for SAC405.

Parameter	Description	Values
s_0 (MPa)	Initial value of state variable, s	As below
Q/R (K)	Activation energy term	10750
A (s^{-1})	Pre-exponential factor	11089
ζ	Stress multiplier	20.986
m	Strain rate sensitivity of stress	0.8793
h_0 (MPa)	Hardening coefficient	As below
$\hat{s}$ (MPa)	Coefficient for deformation resistance saturation value	60.173
n	Strain rate sensitivity of the saturation value	-7.0368×10^{-7}
a	Strain rate sensitivity of the hardening coefficient	2.0110

$$s_0 = 26.76 + 0.04586T - 5.4317 \times 10^{-5}T^2$$

$$h_0 = 62.84 - 506.35T + 4.172T^2 - 1.4788 \times 10^{8}\dot{\varepsilon}_{in} - 1.1169 \times 10^{5}{\dot{\varepsilon}_{in}}^2$$

Once the Anand parameters were determined, the model can be used to predict the stress-inelastic strain curve at a particular temperature and inelastic strain rate. The reliability of the model is evaluated by comparing the stress-inelastic strain curves of the experimental test in terms of the goodness of fit between the model and test data. Figure 1 and Figure 2 shows a comparison between the predicted model and experiments at various inelastic strain rate and temperature, respectively. In most cases, good correlation is obtained indicating that the extracted parameters provide a good fit to the experimental data. However, at 10^{-3} s^{-1} and 150°C curve, the goodness of fit (R^2) is around 70%. This is due to the calculated saturation stress being slightly lower compared to the experimental data which is 25.0 MPa instead of 26.7 MPa. The problems may arise from the process in determining the temperature and inelastic strain rate dependent parameters, such as s^*. This problem may be solved by building a correlation between the parameters representing the influence of strain rate and temperature with these conditions appropriately.

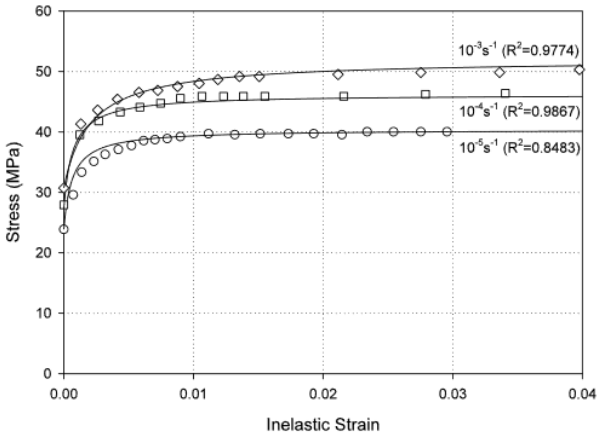

Figure 1 Numerical and experimental stress-inelastic strain curves for SAC405 at 25°C with 3 different inelastic strain rates.

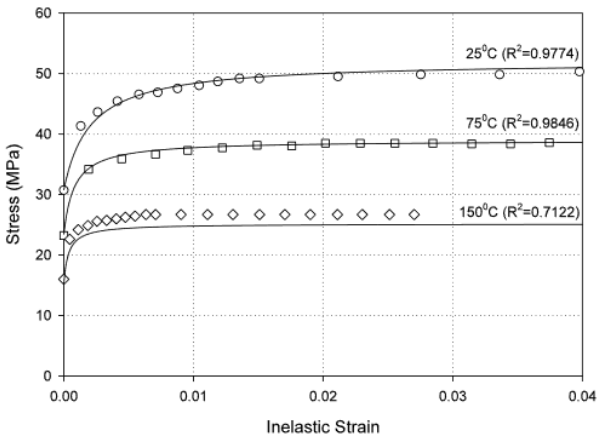

Figure 2 Numerical and experimental stress-inelastic strain curves for SAC405 at 10^{-3} s^{-1} with 3 different temperatures.

5. CONCLUSION

A unified constitutive model Anand is largely used to predict the inelastic behavior of SAC405 solder material. By using optimization techniques and a series of tensile tests with various temperature and strain rate, the model parameters are determined. Results show that a modified Anand model can capture the flow stress and especially at the low inelastic strain. A good comparison was found between test data and a numerical model. It illustrates that the model can predict the flow stress and inelastic strain over a wide range of temperatures and inelastic strain rates.

REFERENCES

[1] Anand, L. (1985). Constitutive equations for hot-working of metals. *International Journal of Plasticity*, *1*(3), 213-231.

[2] Brown, S. B., Kim, K. H., & Anand, L. (1989). An internal variable constitutive model for hot working of metals. *International Journal of Plasticity*, *5*(2), 95-130.

[3] Chen, X., Chen, G., & Sakane, M. (2005). Prediction of stress-strain relationship with an improved Anand constitutive model for lead-free solder Sn-3.5 Ag. *IEEE Transactions on Components and Packaging Technologies*, *28*(1), 111-116.

[4] Qiang, W., Lihua, L., Xuefan, C., Xiaohong, W., Liu, Y., Irving, S., & Luk, T. (2007, April). Experimental determination and modification of Anand model constants for Pb-free material 95.5 Sn4. 0Ag0. 5Cu. In *2007 International Conference on Thermal, Mechanical and Multi-Physics Simulation Experiments in Microelectronics and Micro-Systems. EuroSime 2007* (pp. 1-9).

Feature identification from product reviews for product evaluation modeling

Syaza Athirah Ramli, Soon Chong Johnson Lim*, Ming Foong Lee

Faculty of Technical and Vocational Education, Universiti Tun Hussein Onn Malaysia, 86400, Parit Raja, Batu Pahat, Johor, Malaysia.

*Corresponding e-mail: scjohnson.lim@gmail.com

Keywords: Product review; feature identification; product evaluation modeling

ABSTRACT – Product evaluation concerns the consumer satisfaction on a product being used, which is essential for quality improvement purpose. Nowadays, users are willing to share their product experience online through product reviews. This study aims to discover important features from product reviews for evaluation modeling. With the focus on phone camera, review documents for two distinctive phones were downloaded from two websites. Salient product features and their corresponding textual descriptions were manually identified and tagged. Product models were also constructed using ontology for analysis at later stage. We report our outcomes in this paper with some indications for further work.

1. INTRODUCTION

Product evaluation is an important study in product design, especially when it involves consumer satisfaction of a product being used that affects perceived product quality. Therefore, in order to produce a product that can meet the needs of consumers, salient features that users emphasized in a product should be identified. Operations of designing a product indirectly involve constantly changing market needs and requirements from time to time. Therefore, product designers should be aware of the latest design trends in accordance with the current technological development to meet with the needs of users [1]. User requirements in this context refer to users' needs to be resolved and also the characteristics and specifications envisioned by the user themselves.

Production of quality products is important to ensure product marketability. Thus, there is a pressing need to manufacture products that meet the contemporary needs of consumers. Product design that is timely is crucial for market success. Therefore, product evaluation needs to be conducted to manufacture products that suite mass user requirements. From previous literature, method such as Analytical Hierarchy Process (AHP) is commonly used for product evaluation. However, problem definition using AHP can be unclear due to the ambiguous oral expression during the decision making process [2].

Nowadays, users shared their experience on the product that they have used through online product reviews. These product reviews are used to help researchers gain product features that are emphasized by consumers. From this aspect, there are also research that focused on analyzing various digital sources of customer voices, which includes user social media data using topic modeling and sentiment analysis [3], and Kansei-based customer evaluation based on linguistic represntation [4]. In this study, we wish to explore product evaluation from the perspective of semantic-based product evaluation. In order to perform this, important product features from product reviews should be identified beforehand for product modeling. We report our outcomes of such an activity, from dataset preparation towards the preliminary product evaluation modeling using ontology in this paper.

2. METHODOLOGY

The overall methodology of our work is as described in Figure 1. From Figure 1, The first phase involves the data collection and pre-processing, where relevant product information is extracted from review websites (e.g., review text) and pre-processed, i.e. cleaned and saved in appropriate format. Second phase involves the model building, which includes mainly two tasks: product feature identification & tagging, and model building based on identified features. The first task aimed to determine the salient product features that customers are interested with and followed by building a computational product representation or modeling using these identified features. Upon the model completion, different product models can be better evaluated.

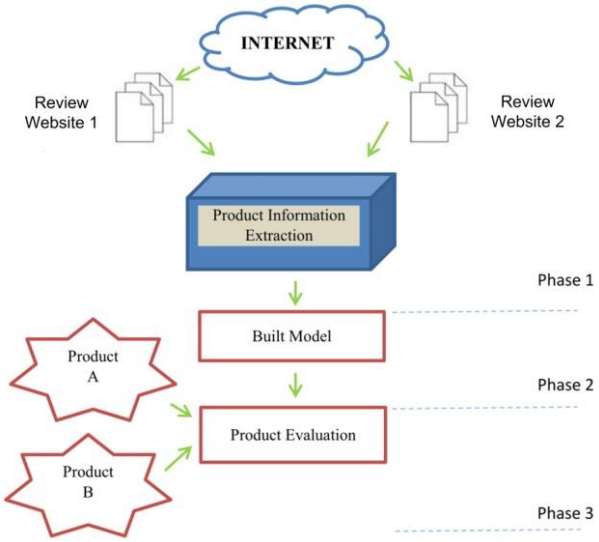

Figure 1 Proposed methodology.

3. RESULTS AND DISCUSSION

Firstly, text-based product reviews information was downloaded from two websites. The product in focus is the camera feature of mobile phones. Two websites are chosen for this purpose, *Amazon* and *DPReview*. Product reviews from *Amazon* represents the views from normal users or amateurs, while *DPReview* represent those users who has higher demands, i.e., professionals. In the context of this study, phone models of year 2015-2017 were preferred because most of these models have larger user base and thus many reviews were available. Two mobile phone models were selected: Apple iPhone 7 Plus and Google Pixel XL. The two popular phone models were selected as there are a lot of reviews available compared to other phone models, thus better details of the two models can be explored. Technically, product reviews are downloaded using specially designed web-scraping script written in the R language. Downloaded data were saved in comma-separated value (CSV) for easier analysis.

Table 1 Summary of product review dataset.

Source	Product	No. of Sentences	No. of Words	No of Tags
Amazon (amazon.com)	Apple iPhone 7 Plus	323	7165	460
	Google Pixel XL	144	4567	426
DPReview (dpreview.com)	Apple iPhone 7 Plus	240	5175	504
	Google Pixel XL	211	4382	336

There are four sets of documents that have been collected: two sets of documents each from *Amazon* and *DPReview*. At this stage, product features were manually extracted and tagged from every review downloaded. The identification for every product feature is in accordance with the features listed in the product specification of a mobile phone. Upon feature identification, tagging of product features is performed where it is aimed to remark important product features in a product review. For instance, HTML-like tags can be used to indicate features identified in the document text. For instance, <f> *optical* </f> can be used to tag a possible important camera feature in a review document. Table 1 presents a summary of the review statistics of downloaded review data and identified tags, with some examples of identified features presented in Table 2.

Table 2 Salient features of amateur user for Pixel XL and iPhone 7 Plus.

Battery	RAM	Processor
Time lapse	HDR	Sound
Snapdragon 821	Mode	Megapixel

Based on the discovered features, computational product representation is built using ontology modeling. Ontology model is an able to model the inherent relationship of product features, enabling rich product information modeling for in-depth semantic-based comparison. For instance, based on product structure, comparison can be performed based on multiple facets of product features. Figure 2 shows an example of a preliminarily completed product ontology model for iPhone 7 Plus.

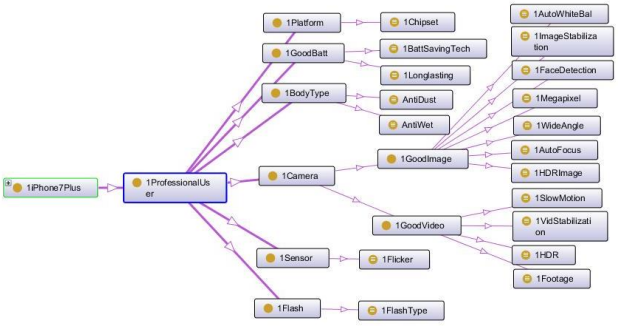

Figure 2 Ontology model for Apple iPhone 7 Plus.

4. CONCLUSION

In this study, a tagged product review dataset that consists of two mobile phones that are collected from two websites is produced. Based on such a tagged data, ontology models for the two mobile phones is constructed to enable analysis at the later stage. In overall, the outcome of the study can be used as a basis for in-depth comparison of products, which is crucial for various purpose of product improvement and competitive analysis.

ACKNOWLEDGEMENT

The work described in this paper was partially supported by a research grant by University Tun Hussein Onn Malaysia under the Ministry of Education, Malaysia (Grant Ref: PPG V023).

REFERENCES

[1] Ceschin, F., & Gaziulusoy, I. (2016). Evolution of design for sustainability: From product design to design for system innovations and transitions. *Design studies*, *47*, 118-163.

[2] Lee, S. H. (2010). Using fuzzy AHP to develop intellectual capital evaluation model for assessing their performance contribution in a university. *Expert systems with applications*, *37*(7), 4941-4947.

[3] Jeong, B., Yoon, J., & Lee, J. M. (2017). Social media mining for product planning: A product opportunity mining approach based on topic modeling and sentiment analysis. *International Journal of Information Management*.

[4] Chanyachatchawan, S., Yan, H. B., Sriboonchitta, S., & Huynh, V. N. (2017). A linguistic representation based approach to modelling Kansei data and its application to consumer-oriented evaluation of traditional products. *Knowledge-Based Systems*, *138*, 124-133.

Mathematical modeling of a simple quarter road vehicle suspension systems on sinusoidal road profile

Adam Samsudin[1,*], Ezzatul Farhain Azmi[2], Amar Faiz Zainal Abidin[1], Mohd Fariduddin Mukhtar[2], Abdul Munir Hidayat Syah Lubis[2], Muhammad Ilman Hakimi Chua Abdullah[2]

[1)] Fakulti Teknologi Kejuruteraan Elektrik dan Elektronik, Universiti Teknikal Malaysia Melaka, Hang Tuah Jaya, 76100 Durian Tunggal, Melaka, Malaysia
[2)] Fakulti Teknologi Kejuruteraan Mekanikal dan Pembuatan, Universiti Teknikal Malaysia Melaka, Hang Tuah Jaya, 76100 Durian Tunggal, Melaka, Malaysia

[*]Corresponding e-mail: adam.samsudin@utem.edu.my

Keywords: Mathematical modeling; suspension systems; road profile

ABSTRACT – Suspension systems have been extensively applied to vehicles. It gives a better ride comfort and road handling to the driver across many type of road profile. A simple mathematical model of a passive quarter car suspension system has been formulated analytical to determine whether the suspension of car model will give a comfortable ride. This study is expected to see the suspension system of heavy road vehicle which is bus and truck model data that are being applied to sinusoidal road profile with considering the basic quarter car model.

1. INTRODUCTION

A suspension system has been applied to vehicles and plays a vital role in order to smooth out the ride while maintaining excellent control. A good suspension system should provide a comfortable ride and good handling within a reasonable range of deflection as previous study [1]. Basically, the function of car suspension system is to keep the car's wheels in firm contact with the road as previous study [2]. This may sound simple, but with acceleration comes force, and forces it to translates into raw energy, when a vehicle accelerates down a road bumps cause forward energy to be converted into vertical energy, which travels through the frame of the vehicle. Without coil and springs to absorb this, vertical energy would cause vehicles to jump up off the road, reduce tire friction and control. Consequently, the car suspension system needs to be investigated and suspension for car also has their potential to improve vehicle performance.

By combining the masses values, the stiffness constant and damping of the quarter car model, it is possible to model any type of road vehicle like car, bus, truck or bicycle.

2. METHODOLOGY

In this study, we formulate a basic quarter car suspension model by a 'sinusoidal road profile'. Numerical solution of 4th order Runge-Kutta methods are used in Maple 13 to solve the suspension system. Where, the result of car suspension system applied to bus and truck for simple model and can be shown graphically.

2.1 Model Analysis

Figure 1 and Figure 2 shows the quarter car model and the force diagram car model where we are able to formulate a mathematical suspension system with satisfying Newton's second law of motion.

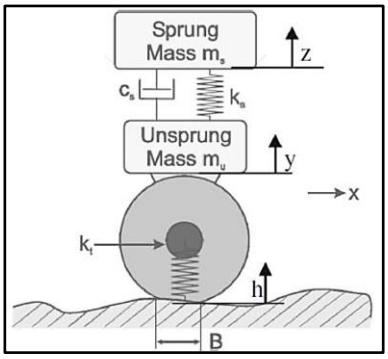

Figure 1 Quarter car model [3].

By applying the Newton's second law of motion, the equations of the simple car motion can be found as in Equation (1).

$$m\ddot{z} + c\dot{z} + kz = kh + c\dot{h} \quad (1)$$

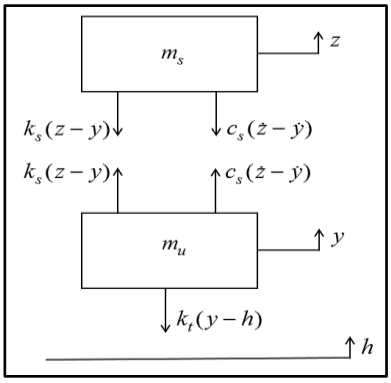

Figure 2 Force diagram of quarter car model.

The equations of the simple car motion can be converted into Equation (2) and Equation (3).

$$m_s\ddot{z} = -k_s(z-y) - c_s(\dot{z}-\dot{y}) \quad (2)$$

$$m_u\ddot{y} = k_s(z-y) + c_s(\dot{z}-\dot{y}) - k_t(y-h) \quad (3)$$

One method of modeling the suspension system is using the general form of the state space model, $\dot{z} = Az + b$. Where z is the vector $[\, z\ y\ u\ v\,]^T$ and b = $[\, 0\ 0\ 0\ kh\,]^T$ The state space model is derived as follow:

Taking $\dot{z} = u, \dot{y} = v, \dot{u} = \ddot{z}, \dot{v} = \ddot{y}$ as the state space variable, the state vector will be:

$$A=\begin{bmatrix} 0 & 0 & 1 & 0 \\ 0 & 0 & 0 & 1 \\ -\frac{k_s}{m_s} & \frac{k_s}{m_s} & -\frac{c_s}{m_s} & \frac{c_s}{m_s} \\ \frac{k_s}{m_u} & -\frac{(k_s+k_t)}{m_u} & \frac{c_s}{m_u} & -\frac{c_s}{m_u} \end{bmatrix}$$

The parameters [3] used are as Table 1.

Table 1 Parameters used for bus and truck.

Parameters	Bus	Truck
m_s	4000	4500
m_u	550	650
k_s	320000	570000
c_s	10000	21000
k_t	1700000	3000000

2.2 Sinusoidal Road Profile

Assume that the road vehicle is travelling with an average horizontal speed V and hence that $z = Vt$.

Then, form for y can be expressed as Equation (4) by referring to Figure 3.

$$y = h\sin\left(\frac{\pi Vt}{d}\right),\ \dot{y} = h\left(\frac{\pi V}{d}\right)\cos\left(\frac{\pi Vt}{d}\right), \quad (4)$$

Where: V=14ms^{-1}, d = 2m, h=0.1m

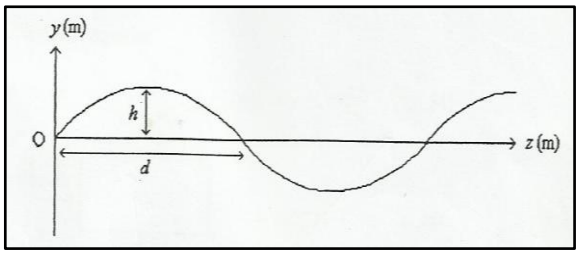

Figure 3 Sinusoidal road profile.

3. RESULTS AND DISCUSSION

The good suspension system should satisfy the prediction by graph [4],

(a) $|z| \leq 0.1$ for all value of time,t.

(b) $|\ddot{z}| \leq 0.6g$ for all value of time,t.

The graph of Figure 4, 5, 6 and 7 indicate that both vertical displacement and acceleration for both bus and truck model shows that it bound implied the prediction I and prediction II.

4. CONCLUSION

In conclusion, the study of heavy road vehicle suspension system on sinusoidal road profile found that this simple car model applied to bus and truck shows both bus and truck fulfilled the prediction to have a good suspension system on sinusoidal road profile.

ACKNOWLEDGEMENT

The authors would like to thank UTeM for funding this work under short Grant Scheme no. PJP/2019/FTKEE3(A)/S01655.

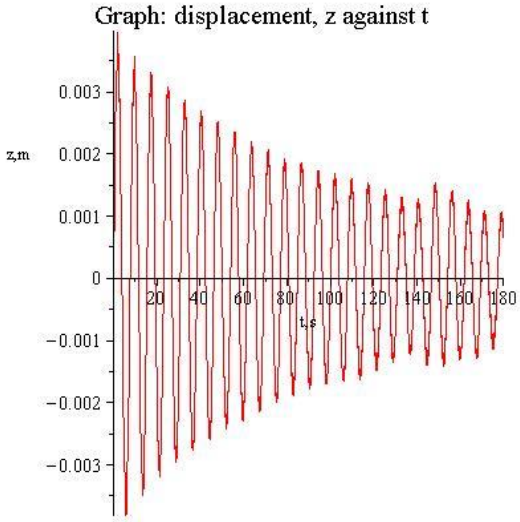

Figure 4 Graph of displacement of Bus z against t.

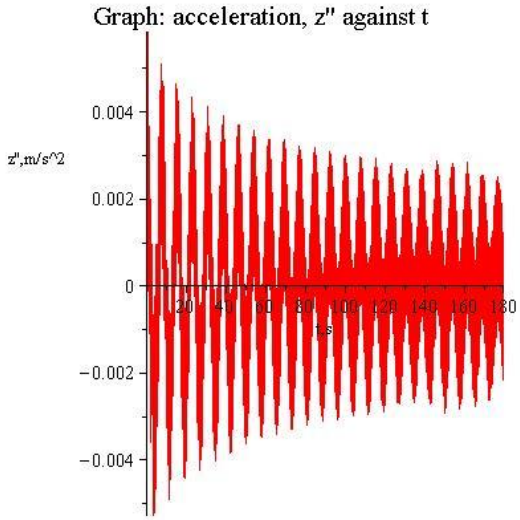

Figure 5 Graph of acceleration of Bus z'' against t.

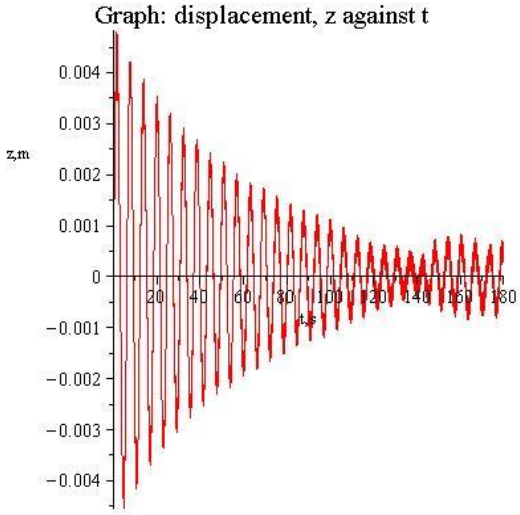

Figure 6 Graph of displacement of truck z against t.

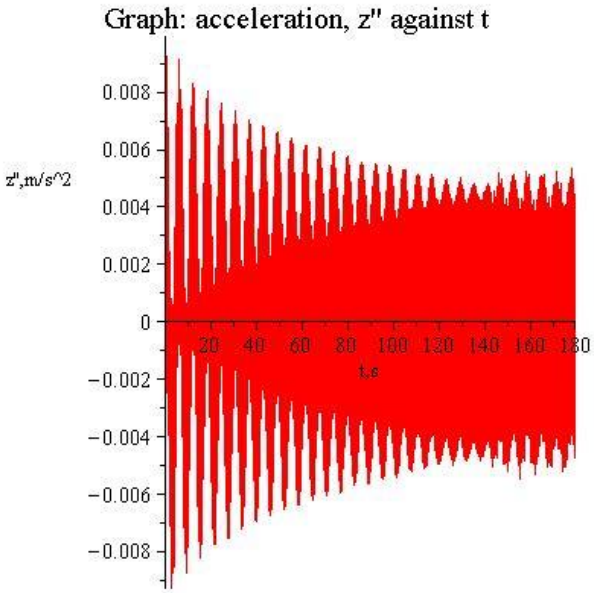

Figure 7 Graph of acceleration of truck z'' againt t.

REFERENCES

[1] Jayachandran, R., & Krishnapillai, S. (2012). Modeling and optimization of passive and semi active suspension systems for passenger cars to improve ride comfort and isolate engine vibration. *Journal of Vibration and control*, 19(10), 1077-5463.

[2] Jha, S. N., Banarjee, S., & Jain, N. (2013). A Textbook of Automobile Technology for Class IX (Level 1). Goyal Brothers Prakashan.

[3] Tejas, P. T. & Modi, M. J. (2016). Mathematical modeling and simulation of a simple quarter car vibration model.*International Journal for Scientific Research & Development*, Vol. 3(11), 2321-0613.

[4] Ahmad, Z. M. A, Shamsuddin, A. & Yeak, S. H. (2017). Mathematical modelling of an electromagnetics automobile suspension. *AIP Conference Proceedings,* 1830, 020051(2017).

Impact of optimization on high-k material gate spacer in DG-FinFET device

Ameer F. Roslan*, F. Salehuddin, A.S.M. Zain, K.E. Kaharudin

Micro and Nano Electronics (MiNE), CeTRI, Fakulti Kejuruteraan Elektronik dan Kejuruteraan Komputer, Universiti Teknikal Malaysia Melaka, Hang Tuah Jaya, 76100 Durian Tunggal, Melaka, Malaysia

*Corresponding e-mail: ameerfarhan@aol.com

Keywords: FinFET; Taguchi; optimization

ABSTRACT – This paper investigates the impact of the high-*K* material gate spacer on short channel effects (SCEs) for the 16 nm double-gate finFET, with output responses optimized using L9 orthogonal array (OA) Taguchi method. Virtual fabrication process and electrical characterization is implemented, and significant improvement is shown towards TiO_2 and HfO_2 material in terms of the I_{ON}/I_{OFF} ratio obtained at 4.0337×10^6 and 3.6089×10^6 for 0.179±12.7% V of threshold voltage (V_{TH}). The I_{ON} from high-*K* materials has proved to meet the minimum requirement by International Technology Roadmap Semiconductor (ITRS) 2013 for high performance Multi-Gate technology for the year 2015.

1. INTRODUCTION

The size of integrated devices reduces day by day with higher demand in multiple operations and therefore, causing size of MOSFETs which is the main component in memory and processors to be scaled down [1]. On top of that, Moore's Law scaling prediction suppression can be done through the proposed new semiconductor devices and applications [2]. The reduction to nanometer regime has triggered the short channel effects to arise which degrades the system performance and reliability. Therefore, a FinFET of 16nm technology is designed along with the performance of the transistor that is improved in relation to the Moore's Law [3]. The devices performance may have been degraded via scaling process for the transistor miniaturization. The short channel effects (SCEs) has affected the device and the performance of the circuit in electron drift characteristics limitation within the channel, besides the reconstruction of the threshold voltage.

Therefore, the gate oxide thickness and the gate-controlled junction or depletion depth in the silicon have to be reduce in proportion to L (Gate Length). Accordingly, alternative structure such as Double Gate FinFET (DG-FinFET) is believed to have solved the scaling problems especially on the device short channel performance and scalability of nanoscale. Appropriate statistical analysis techniques have been implemented to apply the input process parameter optimization from data collected. In fabricating a proper DG- FinFET device, each steps of fabrication and its order have been prioritized. Other than that, in obtaining the desired threshold voltage level (V_{TH}), drive current (I_{ON}), leakage current (I_{OFF}), and sub-threshold swing (SS), several device characteristics is studied and optimized by implementing L_9 orthogonal array (OA) Taguchi statistical method due since the variations of the process parameters may result in variations to the output responses [4].

2. METHODOLOGY

2.1 Virtual Fabrication Process

In this study, ATHENA and ATLAS modules from Silvaco International is used to simulate the fabrication process of DG-FinFET device. Each ATHENA and ATLAS differs in its functionality in which is for process simulation of MOSFET device as shown in Figure 1. By using Device simulation, electrical characteristics of parameters, namely V_{TH}, I_{OFF}, I_{ON} and SS can be extracted. HfO2, Si_3N_4 and TiO_2 both have been used as dielectric materials in the construction of 16 nm DG-FinFET. The device performance has been analyzed in term of V_{TH}, I_{OFF}, I_{ON} and SS and subsequently the ratio of I_{ON}/I_{OFF} by performing variation on gate length, channel doping and S/D doping concentration.

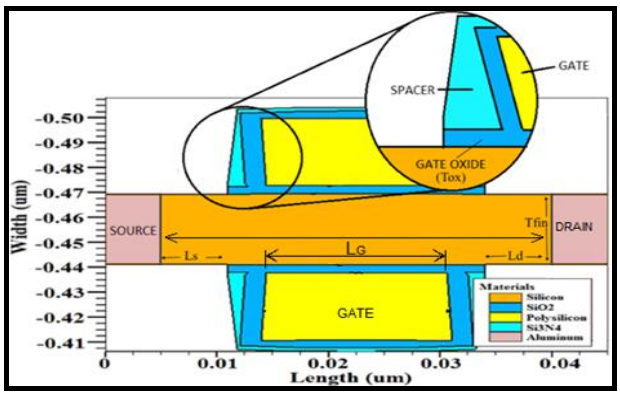

Figure 1 Simulated Structure of the PolySi/SiO_2-based DGFinFET.

2.2 Design of Experiment using L_9 OA Taguchi Method

Based on the parameters identified, the optimization process has been done through variations of process parameter that is identified as in Table 1, along with two levels of noise factor, which is consisting of gate oxidation temperature, Y and polysilicon oxidation temperature, Z of 870ºC and 875ºC to observe the changes towards the output responses in V_{TH}, I_{ON}, I_{OFF} and SS.

Table 1 Process parameter levels for Si_3Ni_4, HfO_2 & TiO_2.

Process Parameters		Unit	Level 1	Level 2	Level 3
V_{TH} Doping Dose	Si_3Ni_4	atom/cm^3	3.85 x10^{13}	3.8 x10^{13}	3.89 x10^{13}
	HfO_2		3.75 x10^{13}	3.77 x10^{13}	3.79 x10^{13}
	TiO_2				
V_{TH} Doping Tilt		deg.	5	6	7
Polysilicon Doping Dose		atom/cm^3	2.10 x10^{14}	2.12 x10^{14}	2.14 x10^{14}
Polysilicon Doping Tilt		deg.	-22	-21	-20

3. RESULTS AND DISCUSSION

3.1 Characteristics of Double Gate FinFET Device

The I-V characteristics is known as the relationship between the electric current through a device and the corresponding voltage across it. The V_{TH}, I_{ON}, I_{OFF} and SS can be extracted from the curve of Drain Current (A) against Gate Voltage (V) from the ATLAS module. Since transistors should have a high I_{ON} and a low I_{OFF} to increase the switching speed of this transistor, the respective output responses are set to have larger-the-best and smaller-the-best for each I_{ON} and I_{OFF}.

3.2 Electrical Characteristic of High-K Dielectric Material

This paper uses the High-K dielectric material from Silicon Nitride (Si_3Ni_4), Hafnium Oxide (HfO_2) and Titanium Oxide (TiO_2) as the gate oxide in 16nm Double Gate FinFET structure. All the devices are set to 0.179±12.7% V based on prediction from ITRS 2013 for high performance (HP) multi-gate technology in the year 2015. This is to precisely evaluate the performance in terms of the corresponding I_{ON}, I_{OFF}, I_{ON}/I_{OFF} ratio, and SS of the aforementioned device. Table 2 shows the comparison between the L9 OA Taguchi method of three different high-K dielectric materials with its best combination settings.

Table 2 Comparison between three different high-K dielectric materials with its best combination settings.

Spacer material		V_{TH} (V)	I_{ON} (mA/μm)	I_{OFF} (nA/ μm)	I_{ON}/I_{OFF} ratio	SS (mV/ dec)
Si_3Ni_4	Initial	0.1871	1916.8725	0.8121	2.3603	93.1799
	Optimized	0.1801	1740.9700	0.6496	2.6840	94.4728
HfO_2	Initial	0.1838	1913.075	0.5818	3.2881	93.8911
	Optimized	0.1811	1840.5975	0.5104	3.6089	93.7842
TiO_2	Initial	0.1851	1961.19	0.5974	3.2829	93.5863
	Optimized	0.1868	1882.35	0.4666	4.0337	93.3385
ITRS Prediction		0.179 ±12.7%	≥1.7	≤100	≥1.48E6	N/A

The FinFET structures spacers is studied by implementing different materials such as Silicon Nitride (Si_3N_4), Hafnium Oxide (HfO_2) and Titanium Oxide (TiO_2) having dielectric constants 7keV, 25keV and 85keV respectively due to its high-*K* dielectric properties. The analysis of the results revealed that the TiO_2 device has superior electrical characteristics compared to others as listed in Table 2.

4. CONCLUSION

In conclusion, the DG- FinFET from simulations have established good electrical properties such as high drive current and low leakage current based on the electrical characteristic analysed. With sufficing V_{TH} that is within the predicted ±12.7% of 0.179V, the TiO_2 and HfO_2 meanwhile have resulting in improvement of the device due to increment towards the I_{ON}/I_{OFF} ratio at respective 4.0337×10^6 and 3.6089×10^6 due to the permittivity of the material alongside the optimization that allows the values of I_{OFF} to be minimized despite lower I_{ON} acquired. That said, TiO2-materialed spacer shows the best I_{ON}/I_{OFF} ratio in conjunction to the device's power consumption efficiency. Besides that, the device characteristics have met the requirement of high performance (HP) multi-gate (MG) technology predicted by ITRS 2013 for the year 2015 requirements.

ACKNOWLEDGEMENT

The authors would like to thank the Ministry of Higher Education (MOHE) for sponsoring this work under project (FRGS/1/2017/TK04/ FKEKK-CeTRI /F00335) and MiNE, CeTRI, Faculty of Electronics and Computer Engineering, Universiti Teknikal Malaysia Melaka (UTeM) for the moral support throughout the project.

REFERENCES

[1] Kaharudin, K. E., Salehuddin, F., Zain, A. S. M., & Abd Aziz, M. N. I. (2015). Optimization of process parameter variations on leakage current in in silicon-on-insulator vertical double gate MOSFET device. *Journal of Mechanical Engineering and Sciences*, *9*, 1614-27.

[2] Panda, S. (2015). *Performance Analysis of Single Gate and Double Gate MOSFET with and without Effect of Noise* (Doctoral dissertation).

[3] Ilatikhameneh, H., Ameen, T., Novakovic, B., Tan, Y., Klimeck, G., & Rahman, R. (2016). Saving Moore's law down to 1 nm channels with anisotropic effective mass. *Scientific reports*, *6*, 31501.

[4] AH, A. M., Menon, P. S., Ahmad, I., ZA, N. F., Zain, A. M., Salehuddin, F., & Sayed, N. M. (2018). Threshold voltage and leakage current variability on process parameter in a 22nm PMOS device. *Journal of Telecommunication, Electronic and Computer Engineering*, *10*(2-8), 9-13.

The vortex shedding for an inclined flat plate of thrombosis using CFD simulation

Nursyaira Mohd Salleh[1], Mohamad Shukri Zakaria[1,2,*], Mohd Juzaila Abd Latif[1,3]

[1)] Fakulti Kejuruteraan Mekanikal, Universiti Teknikal Malaysia Melaka,
Hang Tuah Jaya, 76100 Durian Tunggal, Melaka, Malaysia
[2)] Centre for Advanced Research on Energy, Universiti Teknikal Malaysia Melaka,
Hang Tuah Jaya, 76100 Durian Tunggal, Melaka, Malaysia
[3)] Advanced Manufacturing Centre, Universiti Teknikal Malaysia Melaka,
Hang Tuah Jaya, 76100 Durian Tunggal, Melaka, Malaysia

[*]Corresponding e-mail: mohamad.shukri@utem.edu.my

Keywords: Flat plate; vortex shedding; CFD; thrombosis

ABSTRACT – The formation of blood clotting due to the combination of vortex shedding that effect by recirculation at the sinus and leaflet. Blood clotting also known as a thrombosis that cause by the non-physiological flow through leaflet of mechanical heart valve (MHV) which lead to high stress and high residence time. This research presents the computational fluid dynamics (CFD) simulation using ANSYS FLUENT 16.1 software to investigate the fundamental knowledge of vortex shedding for inclined flat plate that reacts as a leaflet on MHV which responsible of thrombosis. The simulation flow at different phase of vortex shedding cycle show different development and shedding mechanism for the two train of vortices in the vortex stress which has different vortex strength. This, paper also determine the mechanism of the fluctuating lift and drag on the plate thus relationship with the vortex shedding.

1. INTRODUCTION

The potential complication in mechanical heart valve MHV system is thrombosis which necessitates chronic systemic anticoagulation after heart valve replacement [1]. Thrombosis is the presence of a blood clot when activated platelets aggregates with damaged blood element. Then, formation of larger platelet aggregates causes by vortex pairing within the wake that could yield both high shear stress and high residence time compared by single vortex which responsible for blood clotting [2].The recirculation at the sinus and from leaflet produce combination vortex shedding when there are sharp edges in mechanical heart valve design [1]. Figure 1 shows the flow past through leaflet of heart valve during deceleration phase that characterize by periodic vortex shedding (von Karman vortex street) in the wake of the valve leaflets [3]. The angle of attack, α for inclined plate will affect the wake region which dominated by vortices at the trailing edge of the plate. The smaller angle of attack will lead to the smaller of wake width and smaller vortices length scales [4]. Thus, the vortex shedding frequency, f scales with the projected width of the plate normal to the free-stream which strouhal number are approximately constant at $St = fB/U_\infty \approx 0.15$ for $a = 30°$, U_∞ being the free-stream velocity. Then, a high numerical solution is required to capture the details of shed vortex.

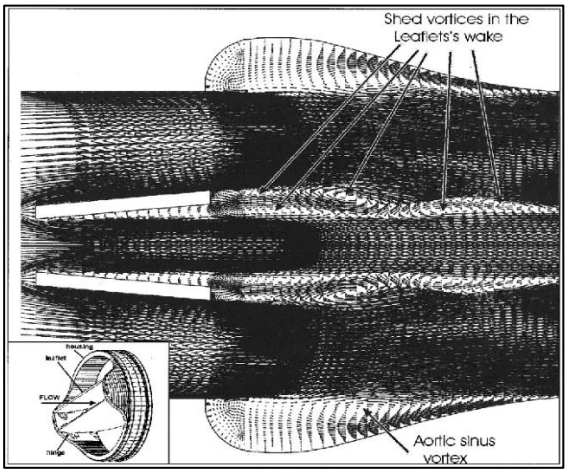

Figure 1 The flow past through leaflet of heart valve during deceleration phase that characterize by periodic vortex shedding (von Karman vortex street) in the wake of the valve leaflets [3].

2. METHODOLOGY

In this study, ANSYS-FLUENT 16.1 software was used to simulate the vortex shedding of 2D flat plate and the geometry was inspired by Lam et al. [4]. The boundary condition at inlet using Reynold number, Re=$U_\infty B/v$ was Re=2x10^4 with the velocity at 2 m/s and width B=15cm. The surface of the plate was then set as solid wall with no-slip condition and the standard wall function. Figure 2 shows mesh of inclined flat plate.

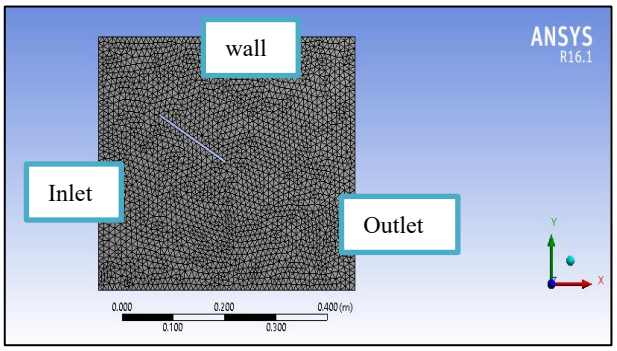

Figure 2 The mesh for inclined plate at α=30°.

The turbulent flow cases with k-ε model was used in physics setup with standard values for model constant;

$C\square$=0.0845, $C1\square$=1.42 and $C2\square$=1.68 [4]. The grid independence test is done by element and node

3. RESULTS AND DISCUSSION

3.1 Vortex Pattern

Figure 3 shows the velocity vector and contour for the inclined flat plate at α=30º. For the solutions of flow velocity, vorticity and pressure at successive phases of a vortex shedding cycle was analyzed to investigate the vortex shedding for inclined flat plate that reacts as a leaflet on MHV that caused the thrombosis. The vortex within the wake indicate to the formation of larger platelet aggregates [5]. Based on Figure 3, the vortex shedding occurs from the two edges of an inclined plate which leading to velocity field in the very near wake which comprises the recirculation region. The wake was found by a train of counterclockwise vortices shed from the trailing edge of the flat plate at the angle of attack, α=30º in the simulation.

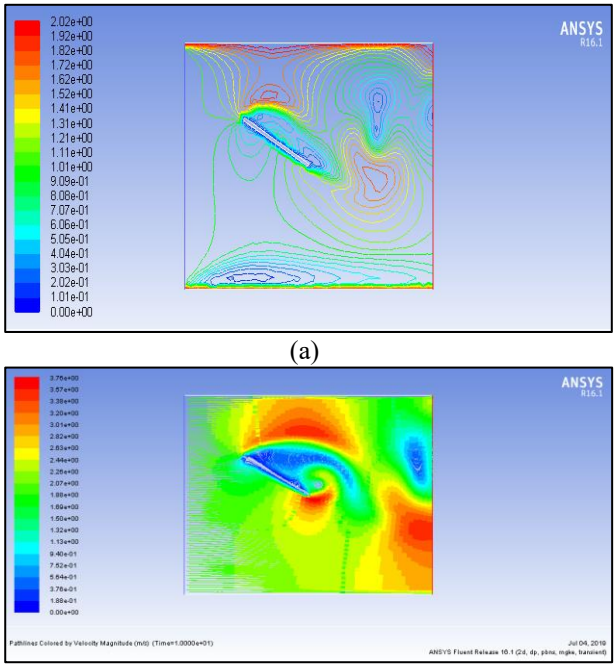

(a)

(b)

Figure 3 The velocity vector of inclined flat plate (a) velocity vector and (b) velocity contour.

3.2 Lift and Drag Coefficients with Strouhal Number

The inclined flat plate was projected to the size of wake width which affected by the angle of attack. The projected plate width B_1= B sin α was shown as a better characteristic length for the wake. The width plate B_1 was used to calculate the Strouhal number for vortex shedding, St= fB_1/U_∞= 0.125. The time history from lift fluctuation was determined as the vortex shedding frequency, f. Figure 4 shows the graph of lift and drag coefficients on inclined flat plate at angle of attack, α=30º.

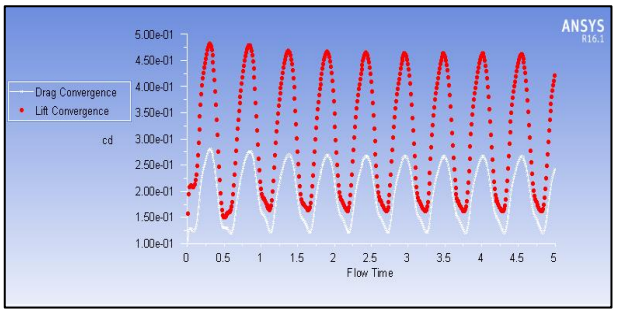

Figure 4 The graph for fluctuating lift and drag coefficients on inclined flat plate at α=30º.

The finding of the graph was according to the previous study by Lam et al. [4] in which lift coefficient is based on projected flat plate width that show less variations with the angle of attack than the lift force. Then, the lift coefficient increased with decreased in angle of attack. Meanwhile the drag on the plate, C_D increased when the angle of attack increased which the projected plate width was used to define the coefficient. The shear layer from the plate leading edge entrains fluid and then produce the suction pressure on upper plate surface which its outward movement leads to lower suction pressure and lower lift and drag force on the plate [7]. The lower shear layer at the plate leading edge indicate to vortex shedding. The bluff body and sharp edge can produce vortex due to inertia [8].

4. CONCLUSION

The vortex shedding phenomenon of inclined flat plate develop blood clotting through lift and drag for angle of attack which indicate the shear layer formation. The recirculation region could increase the shear stress and residence time of the blood thereby contributing to blood clotting. The investigation of vortex shedding on the flat plate at angle of attack, α=30º revealed that the vortex rolling up at leading edge remained attached to the rear of flat plat than trailing edge vortex. However, the present study only acknowledges a single vortex case for flat plate to understand the formation that could increase the shear stress which responsible for blood clotting.

ACKNOWLEDGEMENT

The author would like to thank the facilities provided by Universiti Teknikal Malaysia Melaka and research grant funded from Ministry of Higher Education of Malaysia (FRGS/2018/FKM-CARE/F00367)

REFERENCES

[1] Zakaria, M. S., Ismail, F., Tamagawa, M., Aziz, A. F. A., Wiriadidjaja, S., Basri, A. A., & Ahmad, K. A. (2017). Review of numerical methods for simulation of mechanical heart valves and the potential for blood clotting. *Medical & Biological Engineering & Computing*, *55*(9), 1519-1548.

[2] Bluestein, D., Rambod, E., & Gharib, M. (2000). Vortex shedding as a mechanism for free emboli formation in mechanical heart valves. *Journal of Biomechanical Engineering*, *122*(2), 125-134.

[3] Lam, K. M., & Wei, C. T. (2010). Numerical simulation of vortex shedding from an inclined flat

plate. *Engineering Applications of Computational Fluid Mechanics*, *4*(4), 569-579.

[4] Bluestein, D., Rambod, E., & Gharib, M. (2000). Vortex shedding as a mechanism for free emboli formation in mechanical heart valves. *Journal of Biomechanical Engineering*, *122*(2), 125-134.

[5] Fage, A., & Johansen, F. C. (1927). On the flow of air behind an inclined flat plate of infinite span. *Proceedings of the Royal Society of London. Series A, Containing Papers of a Mathematical and Physical Character*, *116*(773), 170-197.

[6] Luo, S. C., Yazdani, M. G., Chew, Y. T., & Lee, T. S. (1994). Effects of incidence and afterbody shape on flow past bluff cylinders. *Journal of Wind Engineering and Industrial Aerodynamics*, *53*(3), 375-399.

[7] Zhen, T. K., Zubair, M., & Ahmad, K. A. (2011). Experimental and numerical investigation of the effects of passive vortex generators on Aludra UAV performance. *Chinese Journal of Aeronautics*, *24*(5), 577-583.

Development of an integrated vaccine system (IVS) for vaccination healthcare database

Mohd Azrul Hisham Mohd Adib[1,*], Muhammad Shahminan Lukman[1], Nur Hazreen Mohd Hasni[2]

[1)] Medical Engineering & Health Intervention Team (MedEHiT), Human Engineering Group,
Faculty of Mechanical Engineering, Universiti Malaysia Pahang, 26600 Pekan, Pahang, Malaysia
[2)] Family Health Unit, Pahang State Health Department,
Jalan IM 4, 25582 Bandar Indera Mahkota, Kuantan, Pahang, Malaysia

[*]Corresponding e-mail: azrul@ump.edu.my, drhazreen@gmail.com

Keywords: Vaccine; integrated system; database; data storage; computer system

ABSTRACT – Hospital Information System or also recognized as a Healthcare Information System (HIS) is an integrated computer system installed throughout the hospital to expand the hospital clinical and administrative function. Nevertheless, the conservative guide method of recording vaccination information is less organized and problematic to be recovered back. IVS is an integrated information technology system that efforts to address the weaknesses in the conventional method by organizing storage for vaccination information and also mobile application to remind the parents of the next vaccination date. IVS is immobile in the initial development thru positive progress.

1. INTRODUCTION

Albania, Vietnam, Guatemala, Senegal and South Sudan are between the countries that have employed this integrated information technology system on vaccination [1,2]. Immunization Information system (IIS) was established by Albania to support birth and vaccination registration, vaccine stock management, cold chain management, and hostile events management following vaccination [2]. More on IIS, it is an intimate electronic database that is population-based, recording all immunization doses residing in convinced geopolitical areas. The compensations of IIS contain providing the immunization histories that are combined to determine suitable vaccination and also amassed vaccination data for surveillance and program operations to improve vaccination rates and decrease diseases that can be prohibited by a vaccine. By having a consolidated record, it can offer official immunization records for school, camping, and other activities entry necessities. IIS also able to prompt immunization due date, guaranteeing the children to only take the desirable vaccination

The Integrated Vaccine System (IVS) is about storing vaccine intake information in a database by the healthcare organization and recovering the data as a reviewed schedule regarding vaccination dates and information by the parents on an application [3]. The parents would also be informed for the next vaccination date through the application. The objective is to have proper and organized information storage regarding vaccine intake information and also to alert the parents of the vaccination date which is not able to be fulfilled by the conventional manual method.

In Malaysia, this kind of vaccination integrated system has not been established yet [4,5]. For this time being, our Malaysia's authorities under the programme of Immunise4life [6] have developed an application called *MYVaksinBaby*. The application can offer information about vaccines and vaccine-preventable diseases. It provides a list of endorsed vaccines under Malaysia's National Immunization Programme and also additional optional vaccines that can be acquired in private hospitals and clinics [7]. Issues or questions such as the safety of vaccines and vaccination status in Islam are also addressed by the *MYVaksinBaby* application. Other than that, this app is also able to send auto-reminder for the next vaccination date [5].

In this paper, the integrated vaccine system for vaccination healthcare database is well developed for address the weaknesses in the conventional method by preparing storage for vaccination information and also mobile application to prompt the parents of the next vaccination date.

2. METHODOLOGY

2.1 Development of IVS

In the IVS development, the registration form was first created using Bracket software. The script from the registration system was sent into the *phpMyAdmin* database (Figure 1) using php and SQLi coding. The *phpMyAdmin* is the database used to store information such as background information of the parents, date of birth, place of birth, gender, permanent address and babies' details including the vaccination schedule (appointment date, type of vaccine and baby weight) and others.

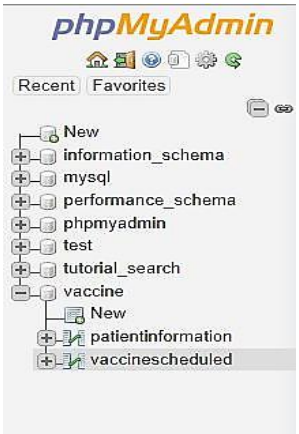

Figure 1 phpMyAdmin database to create the registration form and vaccine database.

2.2 Appearance of IVS

A second database known as IVS interface vaccine database (Figure 2) was created using *phpMyAdmin* as well to connect php in the registration form with the database. The vaccine database consists of two separate tables: a patient information table and the vaccine schedule table (Figure 3). A patient information table is to store all data in the registration form while vaccine schedule table is to record vaccination information of the babies.

Figure 2 IVS interface for "registration purpose.

Figure 3 Vaccine database for patient vaccination schedule.

3. RESULT AND DISCUSSION

3.1 Implementation of IVS

The first step, the parents need to sign up the registration form. All of the compulsory information of the registration form needs to be filled up first before the vaccine schedule table can be generated. By registration, the patients will obtain their own unique ID. After registration, a new appointment date for the next immunization will be set up. The parents will be guided to install a reminder application to remind them of the next vaccination date. The remainder will be triggered one week and one day before the appointment date using the application. In the next vaccination appointments, the patients will go through the same procedure excluding the registration and application installation parts as shown in Figure 4.

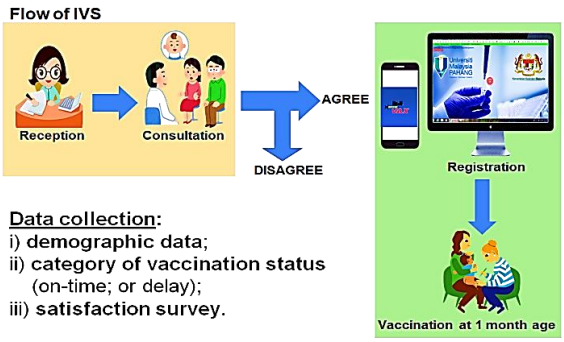

Figure 4 Process flow of implementation the IVS.

4. SUMMARY

As we knew that the IVS development is still in the early stage and so far is presenting the great progress based on the registration form and vaccine database created. For the next progress, the vaccine database will be updated more and the reminder application will be developed.

ACKNOWLEDGEMENT

A big thank you dedicated to University Malaysia Pahang (UMP) for providing us with a good environment and facilities in order to complete this research. By this opportunity, we would like to thank Dr. Siti Suhaila Binti Suradi, MD. from Klinik Kesihatan Kurnia and Dr. Fatimah Binti A. Majid from Pejabat Kesihatan Daerah Kuantan, for sharing valuable information in accordance to our research interest. We would face many difficulties without their assistance.

REFERENCES

[1] World Health Organization (WHO) and Path, Optimize, (2013).

[2] Centers for Disease Control and Prevention (CDC), U.S. Department of Health & Human Services, (2016).

[3] Adib, M.A.H.M., Hasni, N. H. M., Zabudin, N. F., Zabudin, Lukman, M.S. (2018) Enhancing the Integrated Vaccine System (IVS) using *MyKidVAX* Mobile Application. *Proceedings of the 10th National Technical Seminar on Underwater System Technology 2018, Lecture Notes in Electrical Engineering*, 2018, 531-539.

[4] Kim, C., Lee, J., Kim, Y. (2002) Early stage evaluation of a hospital information system in a middle-income country: a case study of Korea. *International Journal of Healthcare Technology and Management*, 4, 514-524.

[5] Zakaria, N., Mohd Yusof, S.A. (2016) Understanding technology and people issues in the hospital information system (HIS) adoption: a case study of a tertiary hospital in Malaysia. *Journal of Infection and Public Health*, 9(6), 774-780.

[6] Immunise4life, Ministry of Health Malaysia, (2016).

[7] Multimedia Super Corridor, Ministry of Health Malaysia, (1997).

Enhanced electron mobility in strained Si/SiGe 19nm n-channel MOSFET device

Ahmad F.N.C. Razak, F. Salehuddin*, Ameer F. Roslan, A.S.M. Zain, K.E. Kaharudin

Micro and Nano Electronics (MiNE), CeTRI, Fakulti Kejuruteraan Elektronik dan Kejuruteraan Komputer, Universiti Teknikal Malaysia Melaka, Hang Tuah Jaya, 76100 Durian Tunggal, Melaka, Malaysia

*Corresponding e-mail: fauziyah@utem.edu.my

Keywords: Strained MOSFET; high-k material

ABSTRACT – In this study, the effects of strain on the 19nm n-channel MOSFET device performance have been investigated. The comparison of performances between unstrained and strained 19nm n-channel MOSFET device was also explored. The virtual fabrication of the device was performed using ANTHENA module while the device's electrical characteristics were simulated using ATLAS module. In this work, higher electron mobility or drive current (I_{ON}) for a device has been achieved by using a high-k material for the gate spacer with Strain Si/SiGe. The result shows that the value of I_{ON} (600 μA/μm) meet the ITRS 2013 prediction for low power performance technology.

1. INTRODUCTION

MOSFET has experienced various changes in improvement. The device continuously scaled down, obeying Moore's Law. Moore's Law states that the feature size transistors are scaled down at a rate of about 0.7 every 18 months [2]. It is estimated that the physical gate length is scaled around 30% for every generation [2]. The reason for scaling down of the MOSFET is to decrease the IC size without downgrading it or to increase the functionality with the same size. The power efficiency also improves as the transistor is scaled smaller and smaller. However, approaching near to 20nm, it becomes more complicated such as SCE to intensify. Shivam et al. [1] informed that by approaching dimension to the nanometer, it had affected the gate leakage current, drain induced barrier lowering and other characteristic parameters arise and the device performance becomes worse. To address this problem, some improvement and changes in device structure and material are needed to provide higher drive current, faster speed, and lower power consumption [1].

Therefore, in this research the performance analysis of single gate n-channel strained with 19nm channel length is studied and investigated. Strained silicon engineering provides higher mobility and helps to reduce power consumption by allowing the use of lower drain voltage (V_{DS}) and higher threshold voltage while maintaining desirable device speed [2/10]. Singh et al. [3/5] mentioned that strained silicon has the potential to achieve high mobility, enhancement in drive current and fit when combining with conventional silicon processing. The researchers also stated that the strain could improve MOSFET drive current by modifying the channel of band structure to enhance the performance even channel length in nanoscale [2,3].

2. METHOD AND MATERIALS

The Strained Si/SiGe 19nm n-channel MOSFET device was fabricated virtually by using ATHENA simulator module. The substrate used for the device was p- type silicon (Si), with a <100> orientation. Then, the device was analysed using ATLAS simulator module. Several electrical characteristics were retrieved from this structure such as threshold voltage (V_{TH}), drive current (I_{ON}), leakage current (I_{OFF}), I_{ON}/I_{OFF} ratio and subthreshold swing (SS). All the values must be compared and met the requirement predicted by International Technology Roadmap Semiconductor (ITRS) for low power (LP) performance single-gate technology [4/ITRS ref]. Figure 1 shows the complete structure of the device where material silicon germanium (SiGe) was acted as a strain and using titanium oxide (TiO_2) as gate spacer. Titanium Oxide (TiO_2) was known as the good material which had the highest permittivity of dielectric constant [5].

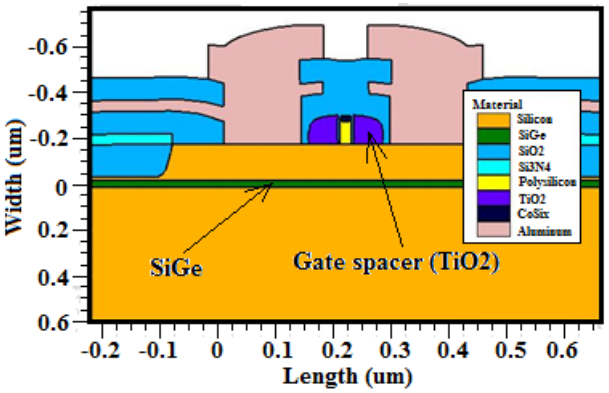

Figure 1 Complete structure of Strained Si/SiGe 19nm n-channel MOSFET device.

Figure 2 shows the characteristic of the Strained Si/SiGe 19nm n-channel MOSFET with TiO_2 material as gate spacer. The two curves in the graph were obtained from the ATLAS simulator module. At the right y axis show a linear scale while on the left y axis shows a logarithmic scale. The number of electrons in the channel increases when the gate voltage (V_G) is increased. The I_{OFF} is at the minimum gate voltage (0V) and the I_{ON} is at the maximum gate voltage (> 1V). The slope of this exponential increase on a logarithmic scale is called the subthreshold slope (*SS*) and is expressed in millivolts per decade of current [6].

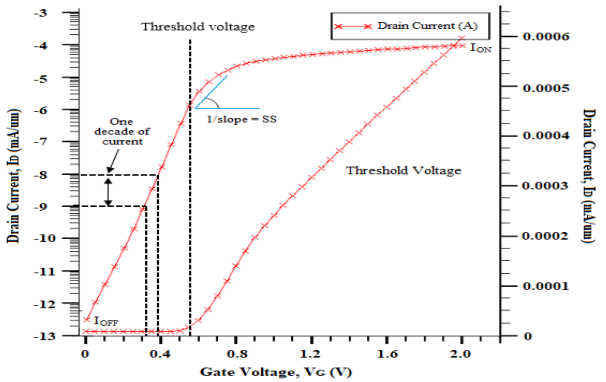

Figure 2 The characteristic of Strained Si/SiGe 19nm n-channel MOSFET with TiO_2 as gate spacer.

3. RESULT AND DISCUSSION

Analysis was performed after the process and device simulation for bulk, silicon on insulator (SOI) and strain 19nm n-channel MOSFET device have been completed. The usage of material doping and the design structure also were considered in this analysis. At the end of the analysis, all results were considered to compare with ITRS and other types of materials. Table 1 shows the comparison between bulk planar and Strain/SOI 19nm single gate MOSFET device with Silicon nitride (Si_3N_4) and TiO_2 as gate spacer.

Table 1 Comparison between bulk planar and Strain/SOI 19nm n-channel MOSFET device.

Electrical Characteristics	ITRS 2013 (For year 2015)	19nm Bulk	19nm SOI with Si3N4 as gate spacer	19nm strain with Si3N4 as gate spacer	19nm SOI with TiO2 as gate spacer	19nm strain with TiO2 as gate spacer
V_{TH} (V)	0.533	0.533	0.532	0.533	0.534	0.533
I_{ON} (μA/μm)	≥ 456	444.7	322.2	363.2	548.8	600.0
I_{OFF} (pA/μm)	≤ 20	450.5	135.5	304.4	113.5	75.4
SS (mV/dec)	70 -90	99.81	85.77	85.51	91.06	80.49
I_{ON}/I_{OFF} ratio	22.8E6	9.9E5	2.4E6	1.19E6	4.84E6	7.95E6

In designing the MOSFET device, technically the transistors should have a high drive current and a low sub-threshold voltage swing in order to increase the switching speed of the device and low power consumption. The optimum value of V_{TH} and minimum leakage current (I_{OFF}) value were the aims to be achieved. The V_{TH} value must in range of ±12.7% as stated in ITRS 2013 [4]. Another parameter that can be considered is subthreshold swing (SS), where with small values of SS will become high value in I_{ON}. Thus, 19nm strain Si/SiGe with TiO_2 as gate spacer give the best value in SS equal to 80.49 mV/decade. It means that an 80.49mV increase in the gate voltage brings about a tenfold increase in the drive current [6].

Meanwhile, the I_{ON}/I_{OFF} ratio shows in term of power consumption. By comparing both tables, Strained Si/SiGe 19nm n-channel MOSFET device with TiO2 as a gate spacer has the highest I_{ON}/I_{OFF} ratio which indicates in less of power consumption. Despite the lower I_{ON}/I_{OFF} ratio of the high-k materials, they have better performance compared to the conventional Si_3N_4. The subthreshold swing is improved as the gate spacer dielectric constant is increased. These results imply that the gate-to-channel control ability is enhanced due to the assistance of the High-k gate spacer dielectric. As a result, a lower leakage current and high driving current for 19nm n-channel MOSFET device can be achieved by using a high-k material for the gate spacer with Strain Si/SiGe. Thereby effectively reducing the power dissipation and increasing the performance of the transistor.

4. CONCLUSION

In conclusion, the Strained Si/SiGe 19nm n-channel MOSFET device has established good electrical characteristics such as high drive current and high I_{ON}/I_{OFF} ratio compare to the bulk planar and SOI MOSFET device. It means strained silicon engineering provides higher mobility and helps to reduce power consumption by allowing the use of lower V_{DS} and higher V_{TH} while maintaining desirable device speed. Besides that, the value of I_{ON} (600 μA/μm) has met the requirement of low power performance single-gate technology predicted by ITRS 2013 for the year 2015.

ACKNOWLEDGEMENT

The authors would like to thank the Ministry of Higher Education (MOHE) for sponsoring this work under project (FRGS/1/2017/TK04/FKEKK-CeTRI/F00335) and MiNE, CeTRI, Faculty of Electronics and Computer Engineering (FKEKK), Universiti Teknikal Malaysia Melaka (UTeM) for the moral support throughout the project.

REFERENCES

[1] Sharma, S., Pundir, A., Pandey, R., Patel, V. K., & Agrawal, N. K. An Analysis of Device Characteristics of Strained N-Channel MOSFET. *International Journal of Electronics and Communication Engineering*, *3*(8), 14-17.

[2] Chaudhry, A., & Sangwan, S. (2013). Modeling of the effect of uniaxial mechanical strain on drain current and threshold voltage of an n-type MOSFET. *Solid-State Electronics*, *79*, 133-137.

[3] Singh, A., Kapoor, D., & Sharma, R. (2017). Performance analysis of SiGe double-gate N-MOSFET. *Journal of Semiconductors*, *38*(4), 044003.

[4] ITRS (2013). www.ITRS2013.net

[5] Ruan, D. B., Chang-Liao, K. S., Li, C. C., Lu, C. C., Liao, Y. L., Chen, L. T., ... & Hsieh, T. L. (2015). Improved electrical characteristics of high-k gated MOSFETs with post-growth treatment on interfacial layer. *Microelectronic Engineering*, *138*, 81-85.

[6] Ferain, I., Colinge, C. A., & Colinge, J. P. (2011). Multigate transistors as the future of classical metal–oxide–semiconductor field-effect transistors. *Nature*, *479*(7373), 310.

The omni-directional of autonomous underwater vehicle (AUV)

Mohd Shahrieel Mohd Aras*, Keek Joe Siang, Grace Wong Mee Sing, Mohd Bazli Bahar, Mohamad Haniff Harun, Ho Gui Yan

Center for Robotics and Industrial Automation (CeRIA), Fakulti Kejuruteraan Elektrik,
Universiti Teknikal Malaysia Melaka, Hang Tuah Jaya, 76100 Durian Tunggal, Melaka, Malaysia

*Corresponding email: shahrieel@utem.edu.my

Keywords: Omni-directional autonomous underwater vehicle; system identification; depth control; pose controller

ABSTRACT – This paper describes development of an Omni-directional movement of an Autonomous Underwater Vehicle (AUV). AUVs needed high maneuverable and responsive to fulfill different underwater tasks in hard-to-reach areas. AUV with an Omni-directional with the configuration of four thrusters which is able to control all six degrees of freedom. Developing an Omni-directional driven using the manual configuration of eight thrusters but only four thrusters will be used. The AUV should be fully holonomic such as it has the ability to control all six degrees of freedom and can perform arbitrary movements in the 3D space while holding any position. The AUV will be developed based on the design parameters then system identification took place once the platform was ready to be tested to get input-output signals. MATLAB System Identification Toolbox is employed to infer the model. Then the model obtained from a toolbox was verified using a fuzzy logic controller This AUV can perform inspection tasks in restricted areas like underwater installations or shipwrecks.

1. INTRODUCTION

Autonomous underwater vehicle (AUV) is commonly known as unmanned underwater vehicle and is a robot that travels underwater without requiring input from an operator. It is an onboard intelligence which a task can be carried out without human operator interference or ship support [1]. AUV is also capable in navigation by following the pre-programmed course. It is suitable in geoscience application which requires constant altitude as the AUV can maintain a linear trajectory through water [2-3]. High maneuverable and agile AUV is needed to fulfill different underwater tasks in hard-to-reach areas. AUV with an Omni-directional with the configuration of four thrusters which are able to control all six degrees of freedom. This project describes its full holonomic control realizing a smooth omni-directional underwater movement. The next steps will be the implementation of different high-level autonomous behaviors, like circle movements around ship hulls in the case of optical investigation missions such as looking for partial damages. The central idea in developing an omni-directional driven AUV using the configuration of four thrusters as shown in Figure 1. Further, the AUV should be fully holonomic such as it has the ability to control all six degrees of freedom (DOF) and can perform arbitrary movements in the 3D space while holding any pose. To perform inspection tasks in restricted areas like underwater installations or shipwrecks, the scale factor has to be small compared to popular underwater robots [4].

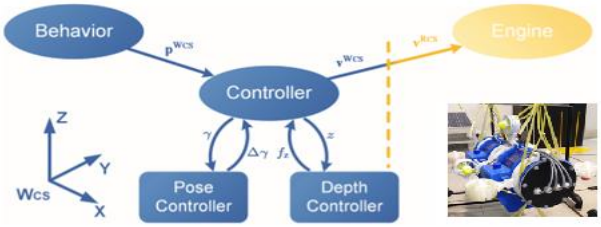

Figure 1 The full holonomic control of AUV.

Beside the construction of the AUV, the full holonomic control of AUV is the second main challenging task. Therefore, a mathematical force model based on the work in [4] is extended to the scenario of the 3D holonomic movement. The control of all six degrees of freedom enables the robot to hold any pose while moving into any direction and is realized with two controllers that is one controller for the depth and one for the pose regulation. The force model as well as the system identification approach. The both models (mathematical and system identification) will be verified.

The full holonomic control of the AUV is subdivided into three parts that is the depth control, the pose control and the movement inside the x-y-plain of the world coordinate system (WCS). Depending on the task, the WCS is given as the inertial measurement unit coordinate system (ICS) without any rotations, such as the yaw, pitch and roll angles between WCS and ICS are assumed to be zero, or it is described by the initial ICS, such as the first pose estimated by the ICS as shown in Figure 1. In such cases, the control of AUV is started when it floats on the water surface and the top of the AUV faces the sky. In the following, this pose is named neutral pose. Further, the ICS is situated in the AUV in a way that its coordinate system directly overlays the AUV coordinate system.

2. METHODOLOGY

For system identification approach, the development of the AUV is considered first and referred as platform development as shown in Figure 1. Generally, the system identification approach consisted of five steps such as (1) design parameter, (2) platform development, (3) system identification technique, (4) model generated based on testing data, and (5) model verification. At step 4, if the model is not good enough, steps 3, 2, or 1 may need to be repeated. The first stage is the design parameter followed by a decision on the design

parameters. The dynamic motion equation must be familiarized. Some of the parameters were obtained from measurement and experiments. After identifying the design parameter, the next stage is the platform development. In this stage, the AUV will be developed based on the design parameters. System identification took place once the platform was ready to be tested to get input-output signals. MATLAB® System Identification Toolbox was employed to infer the model. Then the model obtained from a toolbox was verified using a fuzzy logic controller and also conventional PID controller. MATLAB® command was used to generate transfer function's model from state space method for the designed AUV's model. This model was based on an open-loop model. In, the next step, a controller was designed to follow the set point.

Transfer function (TF): $$G(s) = \frac{Y(s)}{X(s)} \quad (1)$$

$$G(s) = \frac{35.62s+84.32}{s^2+1.027s+0.5668} \quad (2)$$

The evaluation is subdivided into two tests such as the depth control and the pose control. For the first real test scenarios a test pool is used to reduce influences like external drifts. The robot has to adjust the current depth to a desired one while holding the neutral pose over a time period. The target and reached depths are logged in cm and plotted over the time. A depth value of 0cm represents the depth while the robot floats on the surface of the water. Both scenarios emphasize that the approach based on controlling the angle of the pose difference, given in the axis angle representation, and the determined parameter of the proposed controller work very well. For this project, two approaches controller will be implemented that is conventional PID controller and Fuzzy Logic Controller (FLC) as shown in Figure 2.

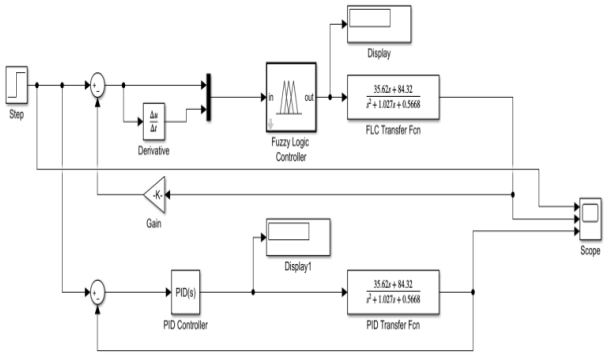

Figure 2: Simulation of depth control of AUV based on system identification model.

3. RESULTS AND DISCUSSION

Figure 3 shows the design of AUV using SolidWorks® software and final hardware of AUV. This AUV consists of eight thrusters that each thruster can be manipulate the configuration of thrusters. In this project only use four thrusters to control of six DOF. The rest thruster as standby mode. All the thrusters can adjust manually to set up configuration as needed.

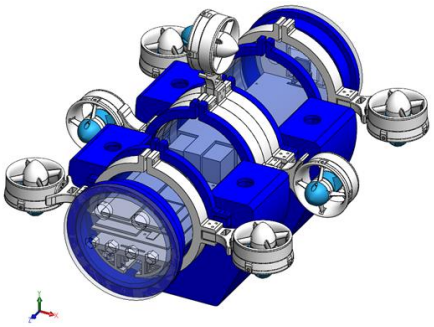

(a) AUV design using SolidWorks software.

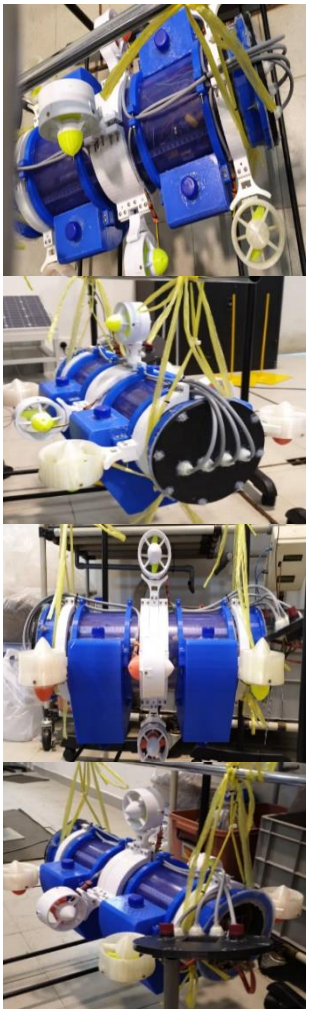

(b) Different view of AUV hardware.

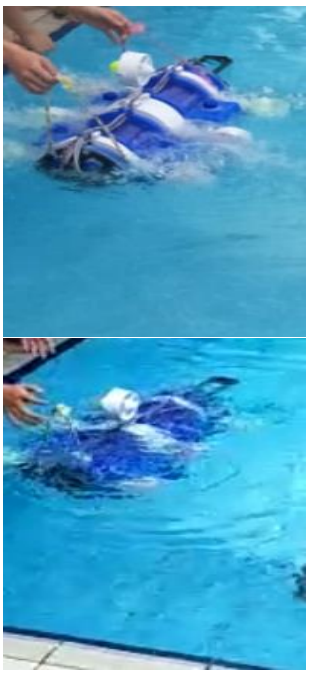

(c) AUV testing on swimming pool.

Figure 3 Autonomous underwater vehicle (AUV).

ACKNOWLEDGEMENT

We wish to express our gratitude and appreciation the support granted by Universiti Teknikal Malaysia Melaka in pursuing this research specially to Underwater Technology Research Group, Faculty of Electrical Engineering, Centre of Research and Innovation Management for supporting this research under PJP (PJP/2019/FKE(3C)/ S01667).

REFERENCES

[1] Aras. M. S. M. (2015). Adaptive simplified fuzzy logic controller for depth control of underwater remotely operated vehicle. *Doctoral dissertation*, Universiti Teknikal Malaysia Melaka.

[2] Rojas, R. (2015). Omnidirectional control. *Robotik*, Freie Universität Berlin, Germany.

[3] Liu, X., Zhang, M., & Yao, F. (2018). Adaptive fault tolerant control and thruster fault reconstruction for autonomous underwater vehicle. *Ocean Engineering*, *155*, 10-23.

[4] Ehlers, K., Meyer, B., & Maehle, E. (2014). Full holonomic control of the omni-directional AUV SMART-E. In *ISR/Robotik 2014; 41st International Symposium on Robotics* (pp. 1-6). VDE.

Quality of Service (QoS) in campus network: Significant survey

Khaled J K Hommouda[1], Zulkiflee Muslim[1,2,*]

[1)] Fakulti Teknologi Maklumat dan Komunikasi, Universiti Teknikal Malaysia Melaka, Hang Tuah Jaya, 76100 Durian Tunggal, Melaka, Malaysia
[2)] Centre for Advanced Computing Technology, Universiti Teknikal Malaysia Melaka, Hang Tuah Jaya, 76100 Durian Tunggal, Melaka, Malaysia

[*]Corresponding email: zulkiflee@utem.edu.my

Keywords: Quality of Service (QoS); Software-Defined Networking (SDN); OpenFlow controller

ABSTRACT – The Internet has provided end-to-end connectivity for users, allowing Quality of Service (QoS) management of network resources for new applications, such as data center, cloud computing, and network virtualization. Although manys solutions have proposed to solve the QoS drawbacks of the recent networking, numbers of them are failed or were not implemented. This paper is to address the comparison between available solutions of QoS in campus network which is related targeted goals of QoS future development in the campus network. The analysis will help future research to decide the best technique to be used in any QoS solution domain.

1. INTRODUCTION

Nowadays, the explosive growth of real-time applications that require stringent Quality of Service (QoS) guarantees, brings the network programmers to design network protocols that deliver certain performance guarantees The objective of the present paper is to get a clear understanding for the Quality of Service (QoS) in campus network obstacles which necessary to address the multiple challenges and realizing the QoS future development for campus networks uses. The effect is represented by attention to the architecture of these networks in which control and the Service (QoS) in the campus network.

2. RELATED STUDY

A role-based SDN campus network slicing approach has been proposed by [1]. The approach involves with authentication controller and the virtualization technology of Flow-Visor which led to reduce the flow setup latency 14% to 60% compared to that of MAC-based slicing. While the proposed approach is required to be applicable in real campus networks to efficiently manage them. A technique for stitching inter-domain paths under the control of centralized routing brokers which known as IXPs has been introduced by [2], it allows for providing paths with end-to-end guarantees for mission-critical applications. A new technique which known as an open northbound API has been proposed by [3]. The method is enables streaming video applications to easily enforce Quality of Service (QoS) requirements in a high-level fashion, without incurring any controller's code coupling or network operator intervention. However, the approach needs to be integrated with other OpenFlow controllers beyond to better support its communication between a single streaming video application and disparate SDN controllers. Another technique of Bandwidth-allocation controller which called (NN-SPID) is developed by [4]. The proposed technique is based on PID control strategy to control QoS requirements relying on an auto-adaptive neural network to ensures the minimum guaranteed bandwidth levels to users according to their contracted SLA, and it also shows more stability and robustness than GA-SPID. However, the proposed technique does not consider on controlling other QoS parameters such as jitter, packet delay of sensitive traffic, or packet loss ratio. In [5] new Scheduling algorithms for evaluating the performance of QoS over MPLS/VPN/WiMAX networks has been presented. Based on the proposed scheduling algorithms, it clearly observed that MWRR has the lowest delay in both VPN and WiMAX. However, the long-term Evolution advanced (LTE-adv) networks have not been achieved yet.

3. METHODOLOGY

The purpose of this systematic review is to classify the literature that is related to our target objectives and create a significant review to identify the most efficient method that is more effective in our research area. In addition to that, challenges and obstacles that were reported in the provided tables which are discussed to identify the problems of the current of campus network framework and related application with Quality of Service (QoS) guaranty approaches (Figure 1).

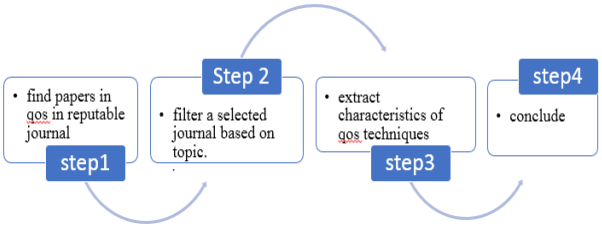

Figure 1 QoS guaranty approaches.

4. ANALYSIS AND RESULTS

After analyzing several papers from several project related to QoS, a comparison was made for a better understanding. Table 1 shows the list of previous projects which had been analyzed and their contribution and drawbacks of their project.

Table 1 Contribution and drawbacks of the previous project.

Technique	Contribution and drawbacks	Ref.
An OpenFlow controller design	A novel approach to stream video over OpenFlow networks with QoS, it fulfilled end-to-end QoS support which is possible with OpenFlow's centralized control capabilities over the network.	[6]
Scheduling mechanism for IMM applications	A new scheduling and channel allocation mechanisms that ensure QoS for IMM applications over WCNs. It delivers QoS with the least handoff delay and minimizes the call dropping probabilities.	[7]
QoS-based Network Virtualization	A constraint placement language used when mapping virtual network (node and links) over the substrate infrastructure to ensure QoS requirements of application flows.	[8]
Optimized Routing in OpenFlow Networks	Streaming setup that utilizes the flexible routing possibilities provided by an SDN implemented with OpenFlow. It improves the QoS by changing the metric model of the Dijkstra algorithm.	[9]
QoS control and SRTP for real-time multimedia streaming	Quality of Service (QoS) control and Secure Real-time Transport Protocol (SRTP) approach to provide a smooth streaming under various network bandwidths, while maintaining effective security.	[10]
A novel SHRP strategy	A novel QoS routing strategy called Swarm-based Hybrid Routing Protocol (SHRP) which able to select the minimum delay path with the maximum available bandwidth at nodes	[11]

Meanwhile, Table 2 is about a summarization about the QoS in respect to Hard and Soft QoS. Each project is defined the metric that being used to evaluate the technique performance.

5. DISCUSSION

The effect of software-defined networks on quality of service of applications is inevitable. Wthe considering the routing methods and metrics used in each of them, one may infer that some novel software techniques and other methods based on Flow Broker architectures are suitable for Quality of Service (QoS) guarantees in networks. In addition, tables above offer a comparison between the most significant methods suggested in the present paper for use of campus networks and other related applications that could be adopted.

6. CONCLUSION

We can conclude that SDN and OpenFlow will most likely become pervasive technologies in the future networks since they have an enormous potential contribution in a large number of different applications and fields. In addition, for QoS in networks, the lack of sufficient bandwidth, as well as high packet loss or delay, can impact very negatively on the quality of service. Finally, more work and focus is needed toward an efficient Quality of Service (QoS) in campus network and related applications is control and guaranty.

REFERENCES

[1] Chen, C. H., Chen, C., Lu, S. H., & Tseng, C. C. (2016, November). Role-based campus network slicing. In *2016 IEEE 24th International Conference on Network Protocols (ICNP)*(pp. 1-6). IEEE.

[2] Kotronis, V., Klöti, R., Rost, M., Georgopoulos, P., Ager, B., Schmid, S., & Dimitropoulos, X. (2016, March). Stitching inter-domain paths over IXPs. In *Proceedings of the Symposium on SDN Research* (p. 17). ACM.

[3] Vasconcelos, C. R., Gomes, R. C. M., Costa, A. F., & da Silva, D. D. C. (2017, January). Enabling high-level network programming: A northbound api for software-defined networks. In *2017 International Conference on Information Networking (ICOIN)* (pp. 662-667). IEEE.

[4] Merayo, N., Juárez, D., Aguado, J. C., De Miguel, I., Durán, R. J., Fernández, P., ... & Abril, E. J. (2017). PID controller based on a self-adaptive neural network to ensure QoS bandwidth requirements in passive optical networks. *Journal of Optical Communications and Networking*, *9*(5), 433-445.

[5] Elkarash, H. H., Elshennawy, N. M., & Saliam, E. A. (2017, December). Evaluating QoS using scheduling algorithms in MPLS/VPN/WiMAX networks. In *2017 13th International Computer Engineering Conference (ICENCO)* (pp. 14-19). IEEE.

[6] Egilmez, H. E., Dane, S. T., Bagci, K. T., & Tekalp, A. M. (2012, December). OpenQoS: An OpenFlow controller design for multimedia delivery with end-to-end Quality of Service over Software-Defined Networks. In *Proceedings of The 2012 Asia Pacific Signal and Information Processing Association Annual Summit and Conference* (pp. 1-8). IEEE.

[7] Alam, M. K., Latif, S. A., Masud, M. H., Akter, M., Anwar, F., & Yalli, J. S. (2013, December). An analysis of scheduling scheme for qos guaranteed interactive multimedia over high speed wireless campus networks. In *2013 1st International Conference on Artificial Intelligence, Modelling and Simulation*(pp. 421-427). IEEE.

[8] Ayadi, I., Diaz, G., & Simoni, N. (2013, October). QoS-based network virtualization to future networks: An approach based on network constraints. In *2013 Fourth International Conference on the Network of the Future (NoF)* (pp. 1-5). IEEE.

[9] Karl, M., Gruen, J., & Herfet, T. (2013, December). Multimedia optimized routing in OpenFlow networks. In *2013 19th IEEE International Conference on Networks (ICON)* (pp. 1-6). IEEE.

[10] Kim, J., Choi, H. J., Lee, S. H., Park, S. H., Song, M. S., & Chang, H. (2013, November). Implementation of quality of service control and security based on real-time transport protocol. In *2013 5th IEEE International Conference on*

Broadband Network & Multimedia Technology (pp. 10-13). IEEE.

[11] Nivetha, S. K., Asokan, R., & Senthilkumaran, N. (2013, July). A swarm-based hybrid routing protocol to support multiple Quality of Service (QoS) metrics in mobile ad hoc networks. In *2013 Fourth International Conference on Computing, Communications and Networking Technologies (ICCCNT)* (pp. 1-8). IEEE.

Table 2 Summary of the QoS in respect to Hard and Soft QoS.

QoS models / Technique	Hard Quality of Service (QoS)				Soft Quality of Service (QoS)			
	Bandwidth	**Delay**	**Jitter**	**Loss**	**Bandwidth**	**Delay**	**Jitter**	**Loss**
New (WIFI AP) mechanism						√		√
Bandwidth controller (NN-SPID)	√				√			
Q-Ctrl system for video flow handling	√				√			
Open northbound API	√	√						
Flow Broker architecture	√	√		√	√	√		√
Role-based SDN campus network slicing						√		
IXPs					√	√		
A (QoE) evaluation model					√	√		
Trust CoS model and Trust DSCP for QoS evaluation					√		√	√
A new QoS mechanisms						√		
Distributed QoS-oriented Model					√	√		
A fine granular API for QoS configuration						√		
A novel software defined automatic QoS management model	√	√			√	√		
Scheduling mechanism for IMM applications					√	√		
New scheduling algorithms						√	√	
A new campus SWAN architecture					√			
QoS-based Network Virtualization					√	√		
Real-time QoS-Aware video streaming					√		√	√
A framework for automatic QoS control	√				√			
Open Cache API					√	√		
Optimized Routing in OpenFlow Networks					√	√		
QoS control and SRTP for multimedia streaming					√	√		
Allocation algorithm with Xen and Linux QoS					√			
Flexible 5G architecture for network slicing					√	√		
A novel SHRP strategy					√	√		

Taguchi GRA for multi-response optimization of16 nm WSi_2/TiO_2 NMOS device

Nor F. Shamsudin[1], F. Salehuddin[1,*], Ameer F. Roslan[1], A.S.M. Zain[1], K.E. Kaharudin[1], A.H. Afifah Maheran[1], I. Ahmad[2]

[1)] Micro and Nano Electronics (MiNE), CeTRI, Fakulti Kejuruteraan Elektronik dan Kejuruteraan Komputer, Universiti Teknikal Malaysia Melaka, Hang Tuah Jaya, 76100 Durian Tunggal, Melaka, Malaysia
[2)] Department of Electronics & Communication Engineering, College of Engineering, Universiti Tenaga Nasional, Jalan IKRAM-UNITEN, 43000 Kajang, Selangor, Malaysia

[*]Corresponding e-mail: fauziyah@utem.edu.my

Keywords: Multi-Response; Taguchi; grey rational analysis

ABSTRACT – In this research, multi response characteristics of 16 nm NMOS device were analyzed using Taguchi GRA. The L_9 Taguchi method, Signal Noise Ratio and ANOVA were used to optimize the effect of process parameters such as Source/Drain and Halo implantation processes. All the simulated values for characteristic are converted to grey relational grade (GRG) and the level of process parameter with the highest GRG are selected as the most optimal level. Most of the results obtained were within the range and met the requirement of low power technology as predicted by ITRS 2013. As a conclusion, the optimization of multi response from the device has been achieved using Taguchi GRA.

1. INTRODUCTION

Scaling down was used to ensure the robust performance of transistor due to the high demand for smaller, faster, and cheaper technology. However, there is some problem to further technology scaling due to the increasing of wafer fabrication process parameter variation. The problem such as short-channel effect (SCE) and drain induced barrier (DIBL) lead to the introducing of high-K material such as Titanium Oxide (TiO_2) [1]. Silicon oxide (SiO_2) has been used as the gate dielectric material over a decade. Nowadays, replacing SiO_2 with high-k material as one of the new research initiatives to overcome those problems. Metal gate such as Tungsten Silicide (WSi_2) is used to eliminate Poly-Si depletion which make the leakage current are too high. This helps in producing better physical and electrical properties of a transistor [2].

In order to obtain the best value of electrical properties of a transistor which is closed to predicted value, several input process parameters are needed. Process parameter plays very important roles in determining the variation. These variations cause significant unpredictability in the power and performance characteristic of integrated circuit [3]. In order to identify the parameter that contribute the most of this variation and get the optimal value of electrical properties, statistically modelling is required. One of the statistical methods for identifying semiconductor process parameters, whose variability would impact most on the device characteristics, is realized using Taguchi method. Taguchi method has become a powerful tool for improving productivity during research and development. However, the application of Taguchi method is only limited to a single response. For multiple response problems, it relies on the decision makers to make judgment and usually leads to a solution that is not globally optimized. Hence, Taguchi method is combined with grey relational analysis (GRA) to solve the multi-response optimization with multiple performance characteristics. A lot of previous reports have employed the Taguchi-based GRA approach to solve multiple objective problems in many engineering fields [4,5].

In this paper, the process parameters of the 16 nm WSi_2/TiO_2 NMOS device were optimized by using Taguchi method with GRA in acquiring a nominal threshold voltage (V_{TH}), a high drive current (I_{ON}) and a low leakage current (I_{OFF}) that meet the requirement of low power technology as predicted by ITRS 2013 [6].

2. METHOD OF THE RESEARCH

The process module starts with wafer preparation followed by well formation, isolation formation, transistor making and interconnection. The wafer preparation includes epitaxial silicon growth, wafer clean and alignment mark etch. Transistor making involves gate oxide growth, high-k deposition, photolithography, metal gate etch, ion implantation and thermal annealing. These are the most crucial process steps in the Integrated Circuit (IC) processing sequences. Several process parameters are needed to obtain the best value of electrical characteristics of the device. In this work, the process parameter that were used are halo implant dose (A), halo implant energy (B), source/drain (S/D) implant dose (C) and S/D implant energy (D). These process parameters will be optimized using Taguchi GRA. Figure 1 shows the 16nm NMOS structure device with TiO_2 as high –k dielectric and WSi_2 as metal gate.

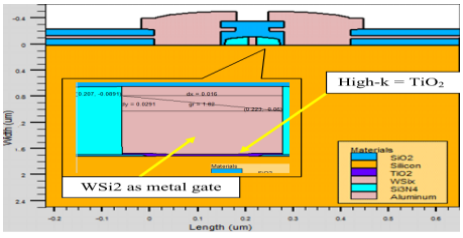

Figure 1 16nm NMOS Structure with TiO_2 as high –k dielectric and WSi_2 as metal gate.

3. RESULTS AND DISCUSSION

Table 1 shows the result of the electrical characteristics based on L_9 OA of Taguchi GRA. The computation for data normalization according to the type of performance characteristics for the device were performed. Then, the deviation sequence was figured before the calculation of the grey relational coefficient (GRC) and grey relational grade (GRG) were computed.

Table 1 Results of the electrical characteristics.

Exp.No.	Process Parameter				V_{TH} (V)	I_{ON} (μA/μm)	I_{OFF} (pA/μm)	I_{ON}/I_{OFF} ratio ($x\ 10^6$)
	A	B	C	D				
1	1	1	1	1	0.5326	507.24	10.20	50.28
2	1	2	2	2	0.5290	513.56	16.67	31.16
3	1	3	3	3	0.5283	513.50	18.66	27.82
4	2	1	2	3	0.5412	484.55	5.604	87.37
5	2	2	3	1	0.5319	509.03	10.56	48.76
6	2	3	1	2	0.5310	508.34	13.15	39.09
7	3	1	3	2	0.5412	485.55	5.038	97.52
8	3	2	1	3	0.5434	479.73	4.498	107.72
9	3	3	2	1	0.5338	504.03	8.441	60.37

The GRC is to represent the deviation of the actual sequence from the desired sequences. The GRG is defined as the average value of all GRCs corresponding to each performance characteristics [7]. Table 2 shows the GRG of process parameters at different levels. Basically, the higher GRG indicated the better overall quality of the design [5]. Table 3 shows the comparison optimum values of V_{TH}, I_{ON}, I_{OFF} and I_{ON}/I_{OFF} ratio characteristics between Taguchi Method and Taguchi GRA.

Table 2 Results for GRG of process parameters.

Symbol	Process Parameters	Grey relational grade (GRG)			Overall mean of GRG
		Level 1	Level 2	Level 3	
A	Halo Implant Dose	0.5219	0.5779	0.7238	0.6079
B	Halo Implant Energy	0.6598	0.6358	0.5281	
C	S/D Implant Dose	0.6279	0.5925	0.6033	
D	S/D Implant Energy	0.5637	0.5904	0.6695	
GRG of optimal levels = 0.8573					

Table 3 Comparison between Taguchi Method and Taguchi GRA.

Condition Description	V_{TH} (V)	I_{ON} (μA/μm)	I_{OFF} (pA/μm)	I_{ON}/I_{OFF} ratio ($x\ 10^6$)
Taguchi Method	0.542	485.66	4.04	120.21
Taguchi GRA	0.547	476.16	3.25	146.51
ITRS 2013 predict for year 2017 [6]	0.530 ±12.7%	≥ 422	≤ 50	8.440

Based on Table 3, V_{TH} was 3.1% higher than ITRS 2013 after the optimization using the Taguchi GRA method but it still in the range of prediction which was between 0.463 V and 0.597 V [6]. Meanwhile, the value of I_{OFF} was decreased by 24.3% after the optimization with Taguchi GRA. In fact, the I_{OFF} was significantly decreased if compared to ITRS 2013 prediction. The I_{ON} value was observed to be decreased by 19.9% after the optimization with Taguchi GRA. However, the I_{ON} value was still above 422 μA/μm as predicted by ITRS 2013 [6]. The I_{ON}/I_{OFF} ratio value after the optimization via L_9 OA of Taguchi-based GRA was increased by 17.9% and higher than ITRS 2013 prediction. Hence, it is concluded that the V_{TH}, I_{ON}, I_{OFF} and I_{ON}/I_{OFF} ratio of the device can be simultaneously optimized using a L_9 OA of Taguchi- based GRA.

4. CONCLUSION

The GRA based on Taguchi method was proposed as a method to optimize multi-response of 16 nm WSi_2/TiO_2 NMOS device. The multiple electrical properties such as V_{TH}, I_{ON}, I_{OFF} and I_{ON}/I_{OFF} ratio were converted into a single multi- performance characteristic, known as GRG. The most optimal values for V_{TH}, I_{ON}, I_{OFF} and I_{ON}/I_{OFF} ratio after the optimization were 0.547 V, 476.16 μA/μm, 3.25 pA/μm and $146.51x10^6$ respectively with 0.8573 of predicted GRG. It can be concluded that the multi response of the device can be simultaneously optimized using a L9 OA of Taguchi- based GRA.

ACKNOWLEDGEMENT

Ministry of Education Malaysia under grant FRGS/1/2017/TK04/FKEKK-CeTRI/F00335. The members of Universiti Teknikal Malaysia Melaka.

REFERENCES

[1] Ruan, D. B., Chang-Liao, K. S., Li, C. C., Lu, C. C., Liao, Y. L., Chen, L. T., ... & Hsieh, T. L. (2015). Improved electrical characteristics of high-k gated MOSFETs with post-growth treatment on interfacial layer. *Microelectronic Engineering*, *138*, 81-85.

[2] Kaharudin, K. E., Salehuddin, F., & Zain, A. S. M. (2018). Optimization of Electrical Properties in TiO2/WSix-based Vertical DG-MOSFET using Taguchi-based GRA with ANN. *Journal of Telecommunication, Electronic and Computer Engineering*, *10*(1), 69-76.

[3] Li, Y., Yu, S. M., & Chen, H. M. (2007). Process-variation-and random-dopants-induced threshold voltage fluctuations in nanoscale CMOS and SOI devices. *Microelectronic Engineering*, *84*(9-10), 2117-2120.

[4] Lin, H. L. (2012). The use of the Taguchi method with grey relational analysis and a neural network to optimize a novel GMA welding process. *Journal of Intelligent Manufacturing*, *23*(5), 1671-1680.

[5] Achuthamenon Sylajakumari, P., Ramakrishnasamy, R., & Palaniappan, G. (2018). Taguchi Grey Relational Analysis for Multi-Response Optimization of Wear in Co-Continuous Composite. *Materials*, *11*(9), 1743.

[6] ITRS (2013). *www.ITRS2013.net*

[7] Kaharudin, K. E., Salehuddin, F., Zain, A. S. M., Aziz, M. N. I. A., Manap, Z., Salam, N. A. A., & Saad, W. H. M. (2016, August). Multi-response optimization in vertical double gate PMOS device using Taguchi method and grey relational analysis. In *2016 IEEE International Conference on Semiconductor Electronics (ICSE)* (pp. 64-68).

Intruder system with raspberry pi in rural areas of Malaysia

Kasthuri Subaramaniam[1,*], Abdul Samad Shibghatullah[1], Harry Lean Fu Liang[1], Zaheera Zainal Abidin[2]

[1)] School of Information Technology, Faculty of Business & Information Science,
UCSI University, 56000 Kuala Lumpur, Malaysia
[2)] Information Security Forensics and Computer Networking (INFORSNET),
Centre for Advanced Computing, Universiti Teknikal Malaysia Melaka,
Hang Tuah Jaya, 76100 Durian Tunggal, Melaka, Malaysia

[*]Corresponding e-mail: kasthurisuba@ucsiuniversity.edu.my

Keywords: Intruder system; Raspberry Pi; rural areas

ABSTRACT – Urban households have better security options compared to rural households. Closed-Circuited Television (CCTV) is a surveillance tool designed to assist in monitoring events. However, the passive monitoring feature of CCTV does not provide any feedback nor respond to the user when a crime incident arises. Thus, a low-cost intruder system with Raspberry Pi which adopts a similar feature and functionality for a home security system is proposed. This is by integrating the feature of the OpenCV library to the Pi Camera to enhance the overall functionality. The use of sensors like a magnetic switch for door and PIR sensors allow the home security system to take in feedback regarding the environment. This will serve as a security layer or enhancement for the home security measurements. The proposed system will help to remedy the passive monitoring feature of CCTV as a smarter and intelligent home security system. The system will be developed in an iteration process and prototyping test will be conducted.

1. INTRODUCTION

Founded by the Raspberry Pi Foundation (UK) the Raspberry Pi computer is a low-cost and high-performance credit card-sized single-board computer that cost around 25 pounds. The Raspberry Pi is designed to teach the younger generation how to program with computers. A single-board computer is referred as a single personal computer board incorporates components such as processor, memory and several types of input and output device that sufficiently to allow it to function as a computer [1]. The credit-card sized Raspberry Pi computer provides alternatives to users to conduct inexpensive and flexible hardware experimentation with programming and electronics.

The rural area is defined as an area which is apart from a city or a non-metropolitan area. Rural is the opposite of urban. In comparison to rural areas, urban areas are usually occupied by a lot of inhabitants, whereas rural area has a smaller number of residents. For instance, rural areas in Malaysia has defined as an area with a population less than 10,000 population, acquire agriculture and natural resources either it is clustered, linear or scattered [3]. The crime rate for property crimes in Malaysia comprises house break-in and theft, vehicles theft, snatch and others. The total property crime cases according to the Department of Statistics of Malaysia (DoSM) is 77,802 cases. With the statistics provided, 21% of the property crime cases come from house break-in and theft [3]. This indicates that an intruder system can be useful in preventing cases like property break-ins and theft.

The Closed-Circuited Television (CCTV) monitoring feature does not provide any feedback nor respond to the user when crime or suspicious incident arise [4]. Using a CCTV as a security system without incorporating the use of sensors can be far less efficient. A modern home security system can provide high efficiency and effectiveness for preventing property theft and break-ins, however subscription to such services is expensive and can cause a burden to household owners in rural areas or urban areas. Thus, a low-cost intruder system with Raspberry Pi which adopts the similar feature and functionality of a modern home security system is proposed.

2. METHODOLOGY

In this proposed system of intruder system with raspberry pi in rural areas will be adopting the prototyping model as the main approach [2]. The prototyping model consists of four (4) stages of development. First, analysis of requirements will be conducted. Approaches or techniques for analyzing the user's requirements and needs can be done via observation or questionnaire. Next, the developer will develop the prototype based on the requirements and needs analyzed from the first stage of prototyping SDLC. Developers then conduct testing on the prototype to ensure it meets the user requirements and needs by involving users in feedback and testing. These two stages are often called the prototype revision or refinement which will repeat until the best version of the prototype is produced. The final product release is achieved when the final version of the prototype produced has met all the user's requirements and needs and it consists of the best efficiency among the prototype version [2].

3. RESULTS AND DISCUSSION

The tables 1 and 2 below shows a brief comparison of the reviewed system and the proposed system [4-8].

The expected contribution of this proposed research is to provide a low-cost security measurement for community household and to reduce the crime rate index of house break-ins in Malaysia. Besides, installing such security measurement for the convenience and protection of the household, owners can also increase the value of

the property. Furthermore, the real-time security updates provide a sense of security for the household owners when they are travelling or not available at home especially in rural areas.

Table 1 Comparison of reviewed and proposed system.

Description	Raspberry Pi	3rd Party Software	Portable	Motion Detection
Smart Home Security with Object Recognition and PIR Sensor	✓	✓	✓	✓
Low-Cost Building Monitoring System (BMS) using Raspberry Pi	✓	✓	✓	
Raspberry Pi Security Camera with Night Vision Capability and PIR Sensor	✓	✓	✓	✓
Smart Home System using Raspberry Pi	✓	✓	✓	✓
Smart Surveillance System using Think Speak and Raspberry Pi	✓	✓	✓	✓
Intruder System with Raspberry Pi in Rural Areas	✓	✓	✓	✓

4. CONCLUSION

In this academic paper, a home intruder system for rural areas has been proposed by adopting the Raspberry Pi technology. The proposed system consists of Raspberry Pi Model 3B+, door sensors, microwave radar sensor and Pi camera with night vision functionality. The overall system includes human detection features and notification system which will alert the household owner once it is triggered by the intruder trespassing the secured parameter. For future research, the plan is to expand the capability of the proposed system such as the accuracy of detection, clarity of image quality and to collaborate with the law-enforcement party to assists in improving the efficiency and effectiveness of crime investigations.

ACKNOWLEDGEMENT

Authors would like to extend their gratitude to CERVIE, UCSI University for funding of the research.

Table 2 Comparison of reviewed and proposed system.

Description	Night Vision	Surveillance Feature	Feedback Feature	Alarm Feature
Smart Home Security with Object Recognition and PIR Sensor		✓		✓
Low-Cost Building Monitoring System (BMS) using Raspberry Pi		✓	✓	
Raspberry Pi Security Camera with Night Vision Capability and PIR Sensor	✓	✓		✓
Smart Home System using Raspberry Pi		✓	✓	
Smart Surveillance System using Think Speak and Raspberry Pi		✓	✓	
Intruder System with Raspberry Pi in Rural Areas	✓	✓	✓	✓

REFERENCES

[1] Raspberry Pi — Teach, Learn, and Make with Raspberry Pi. https://www.raspberrypi.org/. Accessed on 11-Feb-2019.

[2] Isaias, P., & Issa, T. (2015). *High level models and methodologies for information systems* (pp. 1-145). New York, NW: Springer.

[3] Department of statistics malaysia press release. *Dep. Stat. Malaysia, 2016*, 5–9.

[4] Abaya, W. F., Basa, J., Sy, M., Abad, A. C., & Dadios, E. P. (2014, November). Low cost smart security camera with night vision capability using Raspberry Pi and OpenCV. In *HNICEM2014* (pp. 1-6).

[5] Surantha, N., & Wicaksono, W. R. (2018). Design of Smart Home Security System using Object Recognition and PIR Sensor. *Procedia Computer Science*, *135*, 465-472.

[6] Perumal, V. S. A., Baskaran, K., & Rai, S. K. (2017). Implementation of effective and low-cost building monitoring system (BMS) using Raspberry PI. *Energy Procedia*, *143*, 179-185.

[7] Kumar S., & Mehta, N. (2017). Smart home system using BECAMEDA, *8*(2), 1108–1112.

[8] Chandana, R., Jilani, S., & Hussain, S. J. (2015). Smart surveillance system using thing speak and Raspberry Pi. *International Journal of Advanced Research in Computer and Communication Engineering*, *4*(7), 214-218.

Enhancing performance of wireless local area network using channel assignment

Noor Atiqah Fatahurahman[1], Zaheera Zainal Abidin[2,*], Abdul Samad Shibghatullah[3,*], Effendi Mohamad[4]

[1)] Kolej Poly-Tech MARA Batu Pahat, Jalan Gading Emas, Sri Gading, 83000 Batu Pahat, Johor, Malaysia
[2)] Information Security Forensics and Computer Networking (INFORSNET), Centre for Advanced Computing, Universiti Teknikal Malaysia Melaka, Hang Tuah Jaya, 76100 Durian Tunggal, Melaka, Malaysia
[3)] School of IT, Faculty of Business & Information Science (FoBIS), UCSI University, Kuala Lumpur, Malaysia
[4)] Fakulti Kejuruteraan Pembuatan, Universiti Teknikal Malaysia Melaka, Hang Tuah Jaya, 76100 Durian Tunggal, Melaka, Malaysia

[*]Corresponding e-mail: zaheera@utem.edu.my; AbdulSamad@ucsiuniversity.edu.my

Keywords: Wireless LAN; channel assignment; 802.11

ABSTRACT – Wireless Local Area Network (WLAN) has become popular for organisation because of its flexibility and easy to install. The performance of WLAN can be greatly affected due to interference from neighbouring WLAN. In normal 2.4 GHz (802.11b/g/n/ax) WLAN access point has 14 frequency channel and assigning a particular frequency channel to each access point is termed as channel assignment. Efficient channel assignment techniques can improve the performance of WLAN by minimizing the interference from neighbouring access point. This research investigates the performance of WLAN in one private university in Malaysia by assigning 3 types of channel assigment that are Current Channel Assignment (CCA), Non-overlapped Channel Assignment (NCA) and Random Channel Assignment. The research uses OPNET Simulation to evaluate the performance of every type of channel assignment. The result shows RCA is better in terms of throuput and delay compare to CCA and NCA.

1. INTRODUCTION

Nowadays, Wireless Local Area Network (WLAN) has been growing rapidly in the world, especially in business and education institutions. There is much type of wireless technology on the market today such as Institute of Electrical and Electronics Engineer (IEEE) 802.11a, b, g, and n series. This wireless networking technology designed for simple data transfer in the area of 100-300 square feet. This wireless networking technology has replaced the wired network and has now been widely used in education centers such as universities and colleges. This wireless network provides the same capability and speeds compare able to wire 10BASE-T, without the problems associated with set up the wire, drill into walls to install wires or install Ethernet cables throughout an office building at a university and college.

WLAN generally consist of a central point connection called an Access Point (AP). It is the same function as hubs or switches in a star topology-based, traditional wired networks in the local area network. The Access Point (AP) can transmit data between different node of the wireless local area network and it serves as the only connection between wireless LAN and wired LAN. Typically, the Access Point (AP) can handle some number of users within 100 - 300 feet. The current researchers show that coverage optimization become big challenge in deployment of WLAN [1-4]. The researcher proposed a solution to self-optimization coverage performance with adjust the power of each beam AP and Received Signal Strength (RSS) and Signal to Interference ratio (SIR) of the sensor. With this solution, the researchers able to improve the performance of coverage and saving cost.

Overlapping eventually make more users within the same coverage area with some AP. AP placement require different frequency channels between neighboring AP to operate in order to avoid co-channel interference within APs. In addition, to increase capacity, the Access Point (AP) must be assigned the appropriate channels and consumers need to make intelligent decisions about which AP to associate with. Furthermore, the decision on the channel assignment, and unity must be based on a global view of the entire campus WLAN, from the point of view of the individual local clients or AP.

Study of Abbasi et al. [5] show that the importance of the issues channel assignment to minimum availability of orthogonal channel of WLAN. The authors find an efficient method to utilize channel overlap of 2.4 GHz band, was achieve high throughput to minimum interferences within backhaul and directional antennas. The researchers propose channel assignments that have the limited number of channels, the concept to assign the sets of channels to connect in the interference area of each node, where the nodes are works with directional antenna. The study has found that it can decrease the channel interference and increase the throughput.

In a study conduct by Tewari and Ghosh [6], it was shown that the frequency assignment and the association control entertainment be an important role and its should be considered simultaneously to improve the network performance. The researcher uses greedy algorithm that deal with the frequency assignment and the association control to increase the throughput.

2. METHODOLOGY

In order to evaluate the performances of different channel assignment this research proposes 3 types of channel assignment that are Current Channel Assignment (CCA), Random Channel Assignment (RCA), and Non-overlapped Channel Assignment (NCA). The CCA is the current channel assignment that is being used in this case

the university uses Channel 1. The RCA is a random channel assignment where any channel is chosen as long as there is no interference from neighbouring access point. The NCA is the non-overlapping channels designated in WLAN that are channels 1,6 and 11. OPNET simulation will be used to implement the proposed channel assignment. Access Point and wireless network are distributed in service area of 60 feet x 100 feet.

3. RESULTS AND DISCUSSION

Figure 1 shows the delay time for CCA, NCA and RCA for FTP application. The graph shows the delay versus time for three channel assignment scheme technique. Horizontal axis refers to time in second while the vertical axis refers to delay in bit/sec. From the figure it shows CCA have the higher delay compare to NCA and RCA.

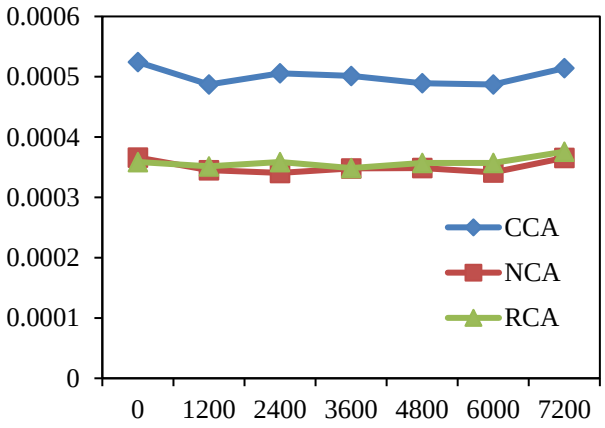

Figure 1 The delay for CCA, NCA and RCA for FTP application.

Figure 2 shows the throughput of CCA, NCA and RCA for FTP application. RCA is the highest in term of throughput compare to NCA and CCA.

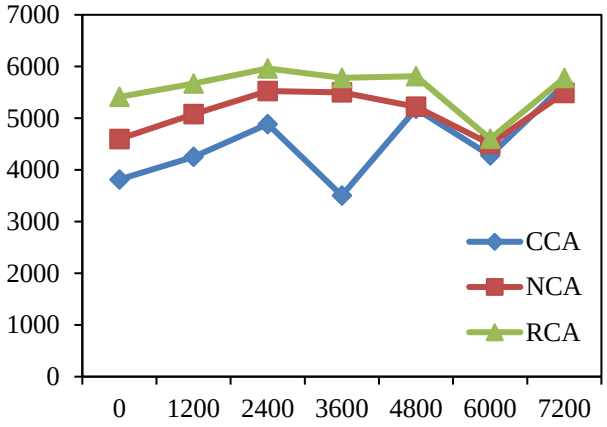

Figure 2 The throughput for CCA, NCA and RCA for FTP application.

Figure 3 shows the average delay in running email application for CCA, NCA and RCA. The results show CCA has the higher delay compare to NCA and RCA.

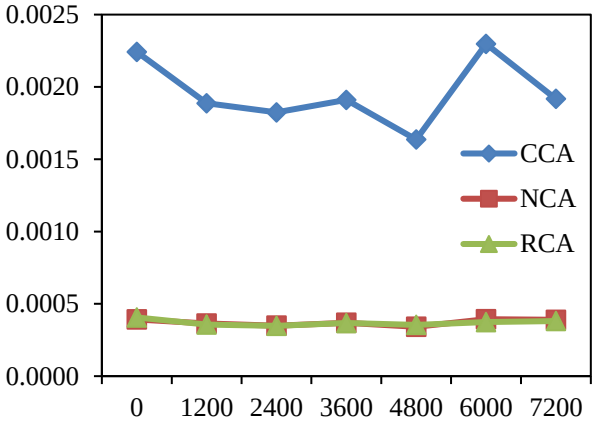

Figure 3 The average delay for CCA, NCA and RCA for email application.

Figure 4**Error! Reference source not found.** shows the throughput in bit/sec for CCA, NCA and RCA for email application. The results show the RCA and NCA are better throughputs compare to CCA.

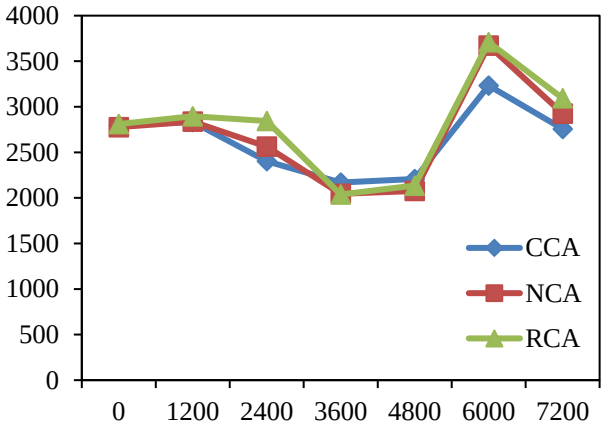

Figure 4 The WLAN throughput for CCA, NCA and RCA for Email application.

4. CONCLUSION

In this paper, two scheme of channel assignment has been proposed on maximizing the performance of WLAN by proposing the non-overlapping channels (NCA) designated in WLAN that are channels 1,6 and 11, and the random channel assignment (RCA). The current or existing channel assignment is CCA. The research used OPNET simulation to evaluate the performance of every scheme of channel assignment for two application that are email and FTP. The results show the RCA is better compare to NCA and CCA.

REFERENCES

[1] Zhou, K., Jia, X., Xie, L., Chang, Y., & Tang, X. (2012). Channel assignment for WLAN by considering overlapping channels in SINR interference model. In *2012 International Conference on Computing, Networking and Communications (ICNC)* (pp. 1005-1009). IEEE.

[2] Arya, L., Sharma, S. C., & Pant, M. (2010). Performance analysis of indoor positioning

system. *International Journal of Advanced Computer Science and Applications*, *1*(4), 37–41.

[3] Chatterjee, S., Sarddar, D., Saha, J., Banerjee, S., Mondal, A., & Naskar, M. K. (2012). An improved mobility management technique for IEEE 802.11 based WLAN by predicting the direction of the mobile node. In *2012 National Conference on Computing and Communication Systems* (pp. 1-5). IEEE.

[4] Choi, J., Lee, K., Lee, S. R., & Ihm, J. J. (2011). Channel selection for IEEE 802.11 based wireless LANs using 2.4 GHz band. *IEICE Electronics Express*, *8*(16), 1275-1280.

[5] Abbasi, S., Kalhoro, Q., & Kalhoro, M. A. (2011). Efficient use of partially overlapped channels in 2.4 GHz WLAN backhaul links. In *2011 International Conference on Innovations in Information Technology* (pp. 7-11). IEEE.

[6] Tewari, B. P., & Ghosh, S. C. (2014). Interference avoidance through frequency assignment and association control in IEEE 802.11 WLAN. In *2014 IEEE 13th International Symposium on Network Computing and Applications* (pp. 91-95). IEEE.

Finite Element Analysis on critical relative slippage of bolted joint under transverse loading

Hairul Bakri[1,2,*], Mohd Adnin Hamidi[3], Mohd Shukri Yob[1,2]

[1)] Fakulti Kejuruteraan Mekanikal, Universiti Teknikal Malaysia Melaka,
Hang Tuah Jaya, 76100 Durian Tunggal, Melaka, Malaysia
[2)] Centre for Advanced Research on Energy, Universiti Teknikal Malaysia Melaka,
Hang Tuah Jaya, 76100 Durian Tunggal, Melaka, Malaysia
[3)] Fakulti Kejuruteraan Mekanikal dan Pembuatan, Universiti Malaysia Pahang,
26600 Pekan, Pahang Darul Makmur, Malaysia

[*]Corresponding e-mail: hairul.bakri@utem.edu.my

Keywords: Critical relative slippage; transverse loading; Finite Element Analysis

ABSTRACT – Critical relative slippage (S_{cr}) is known as a limit before loosening mechanism to occur. This limit is very crucial to predict the performance of bolted joint. Therefore, in this study, investigation of S_{cr} for M10 bolted joint under transverse loading was conducted using finite element (FE) analysis. FE model was validated by comparing the relationship between preload and twisting torque for FE model and theoretical values. S_{cr} values from FE analysis and experimental results were compared and good qualitative agreement was obtained.

1. INTRODUCTION

Nowadays, bolted joint is still relevant as a discussion and research topic since bolted joint is widely used for its low cost in production and producing a high fastening power with low tightening force. In addition, troubles related to loosening and failure of bolt is still occurring. This is an indicator that focus is needed at this joint structure to improve the reliability and its performance.

In this paper, attention is given to study the self-loosening behaviour under transverse loading. This type of loading is said to be the main contributor of failure in bolted joint [1]. According to Junker [2], Pai and Hess [3], the fastening preload immediately decrease by the rotation of nuts if the relative slippage on interface between nut and fastened body goes beyond certain critical limit. This critical limit is called critical relative slippage (S_{cr}) which can be determined by relationship between transverse load and displacement of fastened body.

Therefore, aim of the current study is to provide database related to S_{cr} for bolted joint under transverse loading. FE analysis is used to complete this task due to cost and time limitation and its repeatability. Results of FE analysis is compared to experimental results done by Nishimura et al. [4] for verification purpose.

2. METHODOLOGY

ANSYS 16.0 is used as general purpose FE analysis software to carry out elastic analysis and determine the relationship between transverse loading and displacement of fastened body. Bolt size M10 is used and the specification of M10 is shown in Table 1. Plates are used as fastened body with length, width and thickness are 45 mm, 40 mm and 9 mm respectively. FE model is shown in Figure 1. Lower plate is a fixed plate while upper plate is a movable plate which subjected to 0.5 mm displacement in *x* direction.

Table 1 Specification of M10.

Nominal diameter	Property class	Pitch	U.T.S (MPa)	Standard axial tension (N)
M10	4.8	1.5	392	12732

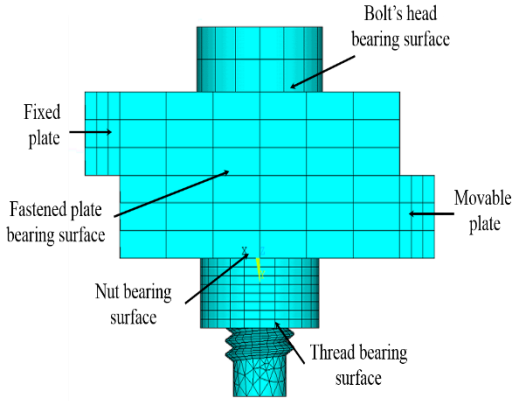

Figure 1 FE model.

Element pair TARGE170 and CONTA174 are used as contact element on bolt head bearing surface, nut bearing surface, fastened plates bearing surface and thread surface. These element pair are suitable for surface to surface contact between three dimensional objects and can deal with Coulomb Friction. Coefficient of friction at all contact surfaces is 0.2 while total number of nodes and elements are 19770 and 7058 respectively.

Fastening preload is generated by slightly shorten the length of body of bolt and permitting its interference movable plate under the constrained of the side of nut surface. 3 different fastening preloads are used 8 kN, 10 kN and 12 kN, respectively. Young's Modulus and Poisson ratio are 205 GPa and 0.3 respectively.

To conform the applicability of presented FE model, verification is done by comparing FE model and theoretical values [5] in term of relationship between fastening preload and twisting torque of nut. In addition, cyclic transverse loading experiment done by Yamamoto and Kasei [6] is also used for verification. Both

comparisons showed good qualitative agreement. Therefore, presented FE model can be used to investigate the S_{cr} for M10 bolted joint.

Finally, FE analysis results are compared to experimental results that conducted by Nishimura et al. [4] same settings are set between experiment and FE analysis in order to obtain reliable results.

3. RESULTS AND DISCUSSION

Due to difficulty to obtain values of S_{cr} from quasi-static experimental results, different approach is used to determine S_{cr} by experiment. Cyclic loading experiments were carried out to determine the relationship between preloads (F) and number of cycles (N) for various relative displacement of fastened plates. Then, loosening speeds (dF/dN) were obtained and plotted with various relative displacement of fastened plates to determine S_{cr} as shown in Figure 2 [7]. Besides, Figure 3 shows the relationship between transverse load and relative slippage for FE analysis. S_{cr} for FE analysis results can be used directly from the relationship in contrast to experimental approach. Since S_{cr} is calculated for 1 complete displacement cycle, therefore the real S_{cr} value need to be multiplied by 2 in FE analysis result.

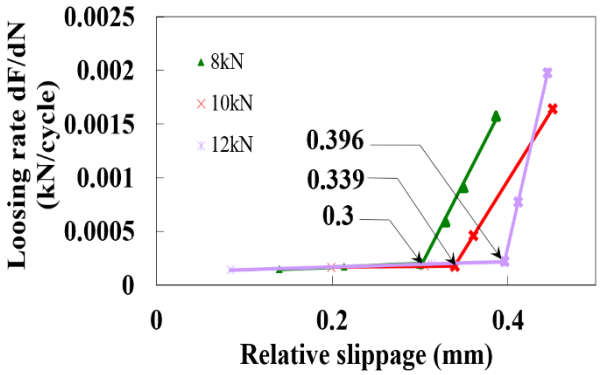

Figure 2 Relationship between fastening preload and relative displacement of fastened plate.

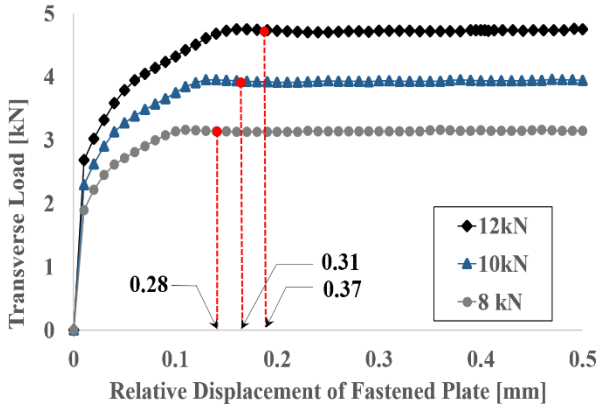

Figure 3 Relationship between transverse load and relative slippage for FE analysis.

Meanwhile, Table 2 shows comparison of Scr values for both FE analysis and cyclic loading experiment. Good qualitative agreements were determined with low percentage of errors between FE analysis and experimental results.

Table 2 Comparison of S_{cr} value.

Fastening Preload (kN)	S_{cr} FE analysis (mm)	S_{cr} Exp. (mm)	Error (%)
8	0.28	0.3	6.6
10	0.31	0.339	8.6
12	0.37	0.396	6.5

4. CONCLUSION

In this presented study, FE analysis was used to investigate the S_{cr} and comparison with experimental method was established for results verification. Therefore, conclusion can be made as following:

(a) Presented FE model is applicable to run FE analysis for bolted joint under transverse loading.

(b) Good qualitative agreements were observed between FE analysis and experimental results. S_{cr} value of FE analysis for preload 8 kN, 10 kN and 12 kN are 0.28, 0.31 mm and 0.37 mm, respectively.

REFERENCES

[1] Bickford, J. H. (2007). Introduction to the design and behavior of bolted joints: non-gasketed joints. CRC press.

[2] Junker, G. H. (1969). New criteria for self-loosening of fasteners under vibration. Sae Transactions, 314-335.

[3] Pai, N. G., & Hess, D. P. (2002). Experimental study of loosening of threaded fasteners due to dynamic shear loads. Journal of sound and vibration, 253(3), 585-602.

[4] Nishimura, N., Hattori, T., Yamashita, M., & Hayakawa, N. (2007). Self loosening behavior of metal thread joints under transverse cyclic loading. In Key engineering materials (Vol. 340, pp. 1467-1472).

[5] Izumi, S., Yokoyama, T., Iwasaki, A., & Sakai, S. (2005). Three-dimensional finite element analysis of tightening and loosening mechanism of threaded fastener. Engineering Failure Analysis, 12(4), 604-615.

[6] Yamamoto, A., & Kasei, S. (1977). Investigations on the Self-Loosening of Threaded Fasteners under Transverse Vibration–A Solution for Self-loosening Mechanism. Journal of the Japan Society of Precision Engineering, 43(4), 470-475.

[7] Yamagishi, T., Asahina, T., Araki, D., Sano, H., Masuda, K., & Hattori, T. (2018). Loosening and sliding behaviour of bolt-nut fastener under transverse loading. Mechanical Engineering Journal, 5(3), 16-00622.

Analysis of SOI PD-MOSFET device using different gate spacer materials

S. Husna S. Hameed, F. Salehuddin*, Ameer F. Roslan, Aida Maziah Manin, Noreazira Mohd Daud, A.H. Afifah Maheran, A.S.M. Zain, K.E. Kaharudin

Micro and Nano Electronics (MiNE), Centre for Telecommunication Research and Innovation, Fakulti Kejuruteraan Elektronik dan Kejuruteraan Komputer, Universiti Teknikal Malaysia Melaka, Hang Tuah Jaya, 76100 Durian Tunggal, Melaka, Malaysia

*Corresponding e-mail: fauziyah@utem.edu.my

Keywords: Silicon on Insulator (SOI); high-k material; PD-MOSFET

ABSTRACT – This project is executed by using Silvaco TCAD software to simulate process and electrical characteristics for the structure of Silicon on Insulator Partially Depleted (PD-SOI) MOSFET that has been designed by following the ITRS 2013. Furthermore, this project facilitates the performance improvement of 19nm SOI PD-MOSFET using high-k material as the gate spacer. Through this project, the device with a SOI layer thickness of 30nm and titanium oxide as the gate spacer yields the highest drive current of 548.78µA/µm and the lowest leakage current of 113.475pA/µm at the threshold voltage of 0.533V compared to other high-k materials as gate spacer and Bulk-Si MOSFET device.

1. INTRODUCTION

Miniaturizing the dimension of Metal Oxide Semiconductor Field Effect Transistor (MOSFET) allows numbers of a transistor to be integrated on a chip. As proofs, in the year 2014, the best Intel processor available contains 1.7 billion transistors while in year 2016, Intel's has well-E CPUs contained 2.6 billion transistors and the high-end Xeon server chips are reported to have more than two billion transistors [1]. Besides, transistor scaling technology gives benefits in reducing the cost per production per single IC, increase the speed and performance, better stability of the operation and less power dissipation of the device. Unfortunately, there are several challenges arise as the device becomes smaller such as performance degradation and short channel effects (SCEs) which make it difficult to continue reducing the device's size follows the conventional law [2]. When downscaling MOSFET, it is hard to maintain a nominal threshold voltage (V_{TH}) as well as reduce the leakage current (I_{OFF}) and subthreshold swing (SS) to improve the device's performance. Therefore, the researchers put their extreme efforts in finding solutions to solve the arising problems. The use of high-k materials and new structure of MOSFET which is known as Silicon-On-Insulator (SOI) technology are then introduced to the semiconductor industry [3]. As what its name imposed, high-k materials have a high dielectric constant (k) which provide improvement of oxide capacitance, less leakage current and better stability to the device operation. Meanwhile, SOI technology refers to a method of depositing a Buried Oxide (BOX) layer on the silicon substrate. It works as an insulating layer to the structure so that when the device is operated, the charge carrier will not be scattered far away from the channel, thus provides a higher speed and a better response of the device. On that account, a new structure of SOI PD-MOSFET device is designed in this project with four different high-k gate spacer materials to increase the drive current hence meet the requirement of high performance.

2. METHODOLOGY

Figure 1 shows one of the structures of 19nm SOI PD-MOSFET with the conventional gate spacer and BOX layer thickness of 30nm. From this figure, the gate length created in the structure is 19nm, the insulating layer thickness shown is 30nm with the Si_3N_4 as gate spacer.

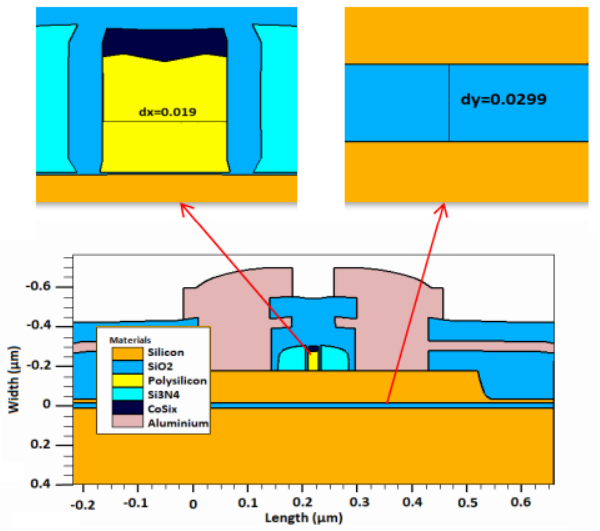

Figure 1 Structure of 19nm SOI PD-MOSFET and Si_3N_4 as the gate spacer.

Throughout this project, Silvaco TCAD software that is commercially available in the industry is used to simulate both fabrication process and electrical characteristics. Silvaco TCAD software consists of two simulators which are ATHENA and ATLAS modules. ATHENA module will be used to simulate the virtual fabrication of SOI PD-MOSFET device while the simulation of electrical characteristics will be implemented using ATLAS module. ATLAS module can produce several graphs such as I_D versus V_G, I_D versus

V_D and log I_D versus V_{DS} to show their electrical behaviour. Four electrical responses that were analysed include drive current (I_{ON}), leakage current (I_{OFF}), threshold voltage (V_{TH}) and the current ratio (I_{ON}/I_{OFF}). After the electrical behaviour is obtained from the simulation, those data are used to be compared with the conventional Bulk-Si MOSFET to prove the performance efficiency.

3. RESULTS AND DISCUSSION

After all the virtual fabrication and device simulation for both Bulk-Si MOSFET and SOI PD-MOSFET designs are completed, those data from ATLAS simulator window are tabulated in Table 1 to ease the comparison.

Table 1 Comparison table for 19nm SOI PD-MOSFET with BOX layer thickness of 30nm.

Condition Description for 19nm MOSFET	V_{TH} (V)	I_{ON} (μA/μm)	I_{OFF} (pA/μm)	I_{ON}/I_{OFF} ratio (x 10^6)
Bulk-Si MOSFET	0.533	444.72	450.50	0.99
SOI with Si_3N_4 as gate spacer	0.533	322.23	135.48	2.38
SOI with Al_3O_2 as gate spacer	0.533	342.78	169.18	2.03
SOI with ZrO_2 as gate spacer	0.533	423.40	154.40	2.74
SOI with HfO_2 as gate spacer	0.533	434.77	150.70	2.88
SOI with TiO_2 as gate spacer	0.533	548.78	113.47	4.84
ITRS 2013 predict for year 2015 [4]	0.533 ±12.7%	≥ 456	≤ 50	9.21

The result obtained from the designed structure of 19nm Bulk-Si MOSFET shown in Table 1 portrays the highest leakage current (I_{OFF}) value of 450.50pA/μm alongside with a value of the drive current (I_{ON}) which is 444.72μA/μm. This result proves the problem of larger leakage current occurs through scaling down planar MOSFET in the semiconductor industry. This is due to the fact that scaling the gate length to 19nm caused the effective channel length to decrease as well and might attach together and cause movement of electrons (leakage current) in the device even though there is no gate voltage being applied [5]. As the gate length is only 19nm, the depletion regions of drain and source merged together as both regions extended, thus causes the punch through inside the device as well. The I_{ON}/I_{OFF} ratio obtained from the result is only $0.99x10^6$ compared to other ratios.

Table 1 shows the expected result is achieved when the TiO_2 is used as the gate spacer for the design of 19nm SOI PD-MOSFET with 30nm BOX layer thickness. This is because TiO_2 with the highest dielectric constant (k=85) helps in enhancing the performance in terms of increase the drive current (I_{ON}) in SOI PD-MOSFET device. As TiO_2 has the highest dielectric constant, it provides higher fringing field that will reduce the barrier height between source and drain in on-state [2]. This design attained a maximum I_{ON} of 548.78μA/μm which is the highest I_{ON} among the other designs (included the 19nm Bulk-Si MOSFET) and the smallest leakage current which is 113.48pA/μm compared to the other MOSFET designs in this project (included the Bulk-Si MOSFET). This result proves that the leakage current and SCE could be reduced by using SOI technology and at the same time the drive current increases when high-k material is used as the gate spacer in the structure. This is in line with the aims stated at the beginning of the project which is to prove that 19nm SOI MOSFET with high-k gate spacer material yields better electrical characteristics compared to the Bulk-Si MOSFET with the same gate length.

4. CONCLUSION

Throughout this project, the 19nm Silicon-on-Insulator (SOI) PD-MOSFETs with four different high-k gate spacer materials are successfully designed with two different BOX layer thicknesses by using ATHENA module while the electrical characteristics for each are analyzed through ATLAS module. Based on the results obtained, it is verified that SOI technology is able to reduce the Short Channel Effect (SCE) and leakage current in the device compared to the Bulk-Si MOSFET, meanwhile the used of high-k gate as the gate spacer is proven useful to improve the performance of SOI PD-MOSFET in terms of both drive current and leakage current.

ACKNOWLEDGEMENT

The authors would like to thank the Ministry of Higher Education (MOHE) for sponsoring this work under project (FRGS/1/2017/TK04/ FKEKK-CeTRI/ F00335) and Faculty of Electronics and Computer Engineering, Universiti Teknikal Malaysia Melaka (UTeM) for the moral support throughout the project.

REFERENCES

[1] Rahman, L. F., Arith, F. B., Idris, M. I. B., Reaz, M. B. I., & Marufuzzaman, M. (2014). Low power in nano-scale CMOS memory. *Journal of Theoretical and Applied Information Technology, 61*(2), 297–303.

[2] Rajneesh S., Rituraj S. R., & Ashwani K. R. (2018). Impact of High-k spacer on device performance of nanoscale underlap fully depleted SOI MOSFET. *Journal of Circuits, Systems and Computers, 27*(4), 1850063.

[3] Kale, S., Banchhor, S., & Kondekar, P. (2015). Performance study of high-k gate & spacer dielectric Dopant Segregated Schottky Barrier SOI MOSFET. *Proceeding of International Conference on Electronics and Communication Systems 2015*, 2015, 1142-1145.

[4] ITRS (2013). *www.ITRS2013.net*.

[5] Chinnappan, U., & Sanudin, R. (2017). Investigation of short channel effects on device performance for 60nm NMOS transistor. *IOP Conf. Series: Material Science and Engineering*, 226(2017), 012143.